Host-parasite interactions of an avian blood parasite elucidated by single-cell transcriptomics

Tim Maximilian Rapp[1], Tobias Lautwein[2], Robert Peuß[3,4], Joachim Kurtz[3,4], Oliver Krüger[1,4], Nayden Chakarov[1,4]

[1]Department of Animal Behaviour, Bielefeld University, Germany

[2]Biologisch-Medizinisches Forschungszentrum (BMFZ), Heinrich-Heine-Universität Düsseldorf, Germany

[3]Institute for Evolution and Biodiversity, University of Münster, Germany

[4]JICE, Joint Institute for Individualisation in a Changing Environment, University of Münster and Bielefeld University, Germany

Correspondence:

Tim Maximilian Rapp

Department of Animal Behaviour

Bielefeld University

Konsequenz 45

33615 Bielefeld

E-mail: timrapp@hotmail.de

Abstract

To date, the intricate cellular and molecular interplay between hosts and parasites is well described for a limited number of model systems. Recent methodological advances now allow deep insights in non-model symbioses, including such that ultimately appear barely antagonistic and may entail intense reciprocal manipulations. We applied single cell RNA-sequencing to blood samples of a wild, long-lived avian host, the Common Buzzard (*Buteo buteo*), infected with the malaria-like parasite *Leucocytozoon toddi*. We identified host cell types and their respective molecular toolkits involved in both, host immunity and parasite virulence. Comparing blood cell-type specific transcriptomic profiles between Buzzards with low and high parasitaemia, we gain insights into the parasitic immune evasion and potential modulation of the host immune response. The response of immune cells was overall low indicating immunosuppression under high parasitaemia, despite the reportedly low pathogenicity of the parasite, likely a result of long-lasting coevolution. Our study illuminates in rare detail a benign host-parasite interaction and bridges a large phylogenetic and symbiotic gap in the evolutionary gradient from parasitism to mutualism. The cell-type specific markers which we identify allow a more complete understanding of the evolutionary forces shaping host immunity.

Key words: Host-parasite interaction, avian malaria, scRNA-seq, transcriptomics, immunosuppression, host response, *Leucocytozoon*, *Plasmodium*

27 Parasites represent a significant proportion of biodiversity and have evolved to manipulate host
28 defences in numerous and diverse ways[1–3]. On an evolutionary scale, this variability of effects ranges
29 from mutualism to parasitism and may be maintained by a trade-off between transmission and
30 virulence[4–9]. Conversely, host immune responses, associated costs and effects on parasites vary
31 strongly among and within species[10]. For example, possible courses of human malaria range from
32 parasite clearance, over asymptomatic and uncomplicated forms, to severe malaria and death[11].

33 The complex lifecycles of intracellular protozoans involve many mechanisms for host cell invasion and
34 immune evasion[12–15]. In well-characterised malaria parasites of the genus *Plasmodium*, some of these
35 mechanisms include antigenic variation, dysregulation of B cells, anergy of T-cells and concomitant
36 immunosuppression[13,14].

37 Despite their long-established role as models of evolutionary ecology, many aspects of the biology of
38 avian malaria and malaria-like parasite remains enigmatic[16]. Here, we focus on *Leucocytozoon*, which
39 is phylogenetically most separated from its haemosporidian sister genera such as *Plasmodium* and
40 *Haemoproteus*[17]. A comparatively high host specificity of *Leucocytozoon* occurs with far more than a
41 hundred different *Leucocytozoon* species, each specialised on a relatively small range of bird species[18].
42 Especially in birds of prey a number of specialist parasite lineages occur, suggesting a long history of
43 co-adaptation between *Leucocytozoon* and their hosts[19].

44 Unlike other haemosporidians, *Leucocytozoon* is capable of infecting diverse hosts cell types, including
45 leukocytes[18]. Furthermore, some *Leucocytozoon* species achieve high prevalence, while displaying
46 apparently low virulence[20–23]. In our study population of Common Buzzards *L. toddi*-infections occurred
47 at prevalences of up to 74% (unpublished data). With its distinct infection biology, high prevalence and
48 evolutionary trajectory, this taxon may allow us annotate a case of rather mutualistic co-adaptation
49 within the wide range of host-parasite interactions.

50 Vector-mediated parent-to-offspring transmission, i.e. quasi-vertical transmission, may facilitate the
51 evolution towards low virulence in *L. toddi*[24,25]. This pattern of transmission might be a pervasive

52 consequence of social niche choice, i.e., territoriality and local confinement of parents and offspring
53 through extended parental care leading to transmission[25,26].

54 The *Leucocytozoon* lifecycle includes merozoite stages invading erythroblasts, erythrocytes, and
55 mononuclear leukocytes within the host. Macro- and microgametocytes ("female" and "male"-type
56 precursors, respectively) then develop in the infected cells. Gametogenesis is initiated upon ingestion
57 by blackflies (Simuliidae)[18]. Nonetheless, the remarkable changes experienced by these parasites
58 throughout their lifecycle have so far never been linked to context-dependent transcriptional changes.

59 Few studies have yet studied transcriptomic responses to haemosporidian infections in wild birds[27–30].
60 However, only whole blood transcriptomes have been analysed potentially convoluting cell-type
61 specific expression changes. Meanwhile, single cell RNA-sequencing (scRNA-seq) became capable of
62 filling this potential gap, with first advances in mapping immune cells in domestic avian species[31–33].
63 Extending the approach to a wild host-parasite system and their blood parasites we identify genes
64 involved in intra- and intercellular interactions between parasite and host cells. By examining the
65 extent of virulence elicited by *Leucocytozoon* we highlight mechanisms potentially driving
66 downregulation of immune genes and a concomitant increase of host tolerance to parasites.

67 Results

68 Identification of 22 distinct cell populations in *L. toddi*-infected peripheral blood

69 A total of 38295 cells were analysed resulting in the identification of 22 clusters via dimensionality
70 reduction of transcriptional profiles (Fig. 1A). A comparison of three HP (high parasitaemia) with three
71 LP (low parasitaemia) samples allowed identification of infected cells (Fig. 1B). Peripheral blood cell
72 type proportions diverged between blood smears and scRNA-seq-derived counts (Tab. S2), indicating
73 a potential bias introduced during cell preparation for scRNAseq (e.g., due to density gradient
74 centrifugation). Overall, 28337 annotated and 712 unannotated genes were detected. Transcript
75 diversity (Fig. S1A), expression levels (normalised UMI counts; Fig. S1B), proportion of mitochondrial
76 and parasite transcripts (Fig. S1C-D, Fig. S2) varied strongly between clusters.

77 **Absence of pronounced changes in immune cell populations**

78 Apart from expectedly strong increases in gametocytes comparing HP versus LP, most other cell types
79 exhibited slightly decreasing proportions (Fig. 1). Signs of adaptive immunity activation, such as clonal
80 expansion of lymphoid cells, were absent. Strong decreases were observed in few cell types such as
81 heterophils and B cells. As indicated above, an increase observed for red blood cells is possibly due to
82 variation during extraction, as highly infected samples have less discrete layering of cell types during
83 density gradient centrifugation.

84 **Strong differential gene expression occurs in two parasite cell types**

85 The differential gene expression analysis resulted in 723 (LP) versus 1278 (HP) DEGs (differentially
86 expressed genes; Fig. 2A, Tab. S4; cut-off value: p-value (adjusted) ≤ 0.05). Overall, 1138 parasite DEGs,
87 866 host DEGs and 29 unannotated DEGs were identified (Tab. S4; cut-off value: p-value (adjusted) ≤
88 0.05). Subsetting the strongest DEGs (cut-off values: p-value (adjusted) ≤ 0.05; $\log_2$-FC (averaged) ≥ 1)
89 limited the pool of genes to 360 DEGs under LP versus 1165 DEGs under HP. The highest number of
90 DEGs was found in microgametocytes and developing gametocytes, while host cells generally
91 expressed fewer DEGs (Fig. 2A-C). Host DEGs were largely expressed under LP, whereas parasite DEGs
92 were predominantly present in HP samples (Fig. 2B & 2C). Since parasite genes dominated under HP
93 in developing gametocytes and the unannotated genes followed the same trend, they likely represent
94 parasitic transcripts. While slightly more of the strongest host DEGs were expressed under LP than
95 under HP, the strongest parasite DEGs were exclusive to HP, but present in all host clusters. This implies
96 an overall downregulation of host transcriptomic responses under HP.

97 A comparison of uninfected versus infected samples was not feasible due to the high prevalence of *L*.
98 *toddi* in the study population during sample acquisition. In order to validate that differential expression
99 analysis of HP versus LP groups represented changes in gene expression related to gradual changes in
100 parasitaemia, we correlated gene expression with parasitaemia as a continuous variable determined
101 from blood smears. The analysis delivered fewer genes of interest with a higher ratio of parasite to

102 host genes. 216 CGs (correlated genes) showed a strong correlation with parasitaemia (Tab. S5, cut-
103 off value: FDR ≤ 0.05). In summary, 182 parasite and 34 host CGs were correlated with the gradient of
104 parasitaemia. The correlations were almost exclusively positive apart from 4 host CGs displaying a
105 negative correlation with parasitaemia in heterophils. Out of the 216 CGs (Tab. S5) 19 parasite genes
106 also represented DEGs retrieved by differential expression analysis (Tab. S4; cut-off value: p-value
107 (adjusted) ≤ 0.05).

108 **Cell-type specificity of DEGs**

109 While we expected to observe cell-type specific host DEGs, parasite gene expression might rely on a
110 more homogenous transcriptomic makeup across cell types, potentially required for the initial invasion
111 of host cells by merozoites. The redundancy of DEGs across clusters was therefore expectedly higher
112 for parasite than for host DEGs (Fig. S6). The most redundant parasite DEGs were only among the top
113 five DEGs under HP in host cells but not in gametocytes (Tab. 1, Fig. S5 & 5).

114 **Immune gene expression generally lacks correlation with parasitaemia**

115 The host immune genes which ranked among the top five DEGs were largely downregulated under HP
116 within various cell types (Tab. 1). These genes are implicated in processes such as in T cell activation,
117 the inflammatory response or pathogen defence (Tab. 1). The strong downregulation of immune genes
118 in various cell types indicates the absence of a pronounced immune response during increasing
119 parasitaemia.

120 Immune effectors including cytokines remained largely unaffected by increased parasitaemia or even
121 displayed downregulation across cell types. Cytokines are crucial for the vertebrate immune response
122 to pathogens[34]. While generally promoting parasite elimination, an exaggerated pro-inflammatory
123 response via TNF-α, IL-6, or IL-8 can also favour severe malaria and pathogenicity[35]. While mostly
124 displaying weak ubiquitous expression, certain cytokines were highly expressed in certain clusters
125 (Tab. S6), but not as significant DEGs (Tab. S6). As an exception, *TGF-β* displayed differential expression
126 under LP in thrombocytes and monocytes.

127 MHC-I components were upregulated under HP in thrombocytes, erythrocytes, T cells and eosinophils
128 (Tab. S6). In contrast, these genes were downregulated under HP in some B cells, T cells and in
129 monocytes (Tab. S6). Interestingly, microgametocytes displayed upregulation of *B2M* (MHC-I
130 component) under HP, while developing gametocytes exhibited the opposite pattern (Tab. S6). MHC-
131 II components were downregulated in a subset of B cells and monocytes under HP (Tab. S6).

132 Among the detectable immunoglobulin mRNAs only *IgL* (*Immunoglobulin light chain λ*) expressed in B
133 cells was significantly diminished under HP (Tab. S6).

134 **Opposing patterns of host gene expression in gametocyte subtypes**

135 PPI-network analysis of host DEGs was conducted to identify pathways responding to parasitaemia.
136 Focusing on developing gametocytes and microgametocytes showing the highest number of DEGs (Fig.
137 3), we retrieved networks with genes partially reoccurring in both clusters, but displaying opposite
138 expression patterns (Fig. 4). The largest group of interactors were components of the ribosome which
139 were downregulated in developing gametocytes, but upregulated in microgametocytes under HP (Fig.
140 4).

141 Discussion

142 This study is the first to perform scRNA-seq on a free-living avian host and its unculturable
143 haemosporidian parasite, demonstrating both the feasibility and opportunities of the method in
144 evolutionary ecology. We focused on changes of host responses to different levels of parasitaemia
145 which are informative about gene expression linked to the severity of infection. Which general
146 patterns can be observed and how do these responses differ between cell types?

147 The annotation of the clusters comprised of *L. toddi* gametocytes based on marker genes led us to
148 subdivide them into putative developing gametocytes, micro- and macrogametocytes. This division is
149 also suggested by the bifurcation of macro- and microgametocyte clusters from the progenitor cell
150 cluster, much like the pattern observed in *P. falciparum*[36]. It is striking that gametocyte subtypes
151 displayed strong differences with regard to basic cellular properties. While general transcript

152 abundance and the ratio of parasite versus host transcripts was highest in macrogametocytes, this
153 cluster simultaneously exhibited the lowest proportion of mitochondrial gene transcripts. The
154 functional differences between micro- and macrogametocytes connected to these alterations in
155 transcript abundance might be linked to differing mitochondrial-to-nuclear genome ratios between
156 *Leucocytozoon* gametocyte types[37]. On the other hand, they are also reminiscent of a mechanism
157 described in *Plasmodium* where maternally derived mRNA-pools drive zygote development[38].
158 Considering the estimated phylogenetic distance of 46-74 million years between *Leucocytozoon* and
159 other haemosporidians the overall weak transferability of *Plasmodium* gametocyte markers is not
160 surprising but complicated the annotation[17]. Conversely, the synergy between our study and diverse
161 scRNA-seq studies on *Plasmodium* can inform about cellular markers and processes which are either
162 common or specific to different groups of blood parasites. For instance, a certain level of conservation
163 between mechanisms controlling macro- versus microgametocyte differentiation in *Plasmodium* and
164 *Leucocytozoon* appears to exist, since we identified an orthologue of *DOZI*, which functions as a
165 translational repressor in macrogametocytes of *Plasmodium*, as a marker of macrogametocytes[38].
166 With the help of such markers, gametocyte ratios might become estimable based on gross blood
167 transcriptomic data.

168 Classically, gametocytes of *Leucocytozoon* are thought to develop within erythroblasts, erythrocytes,
169 and mononuclear leukocytes[18]. On the other hand, it has more recently been suggested that some
170 Leucocytozoon species solely infect thrombocytes, while other species seem to differ in their host cell
171 choice[39–41]. Likewise, the overall similarity of transcriptional profiles between gametocytes and
172 thrombocytes also points to thrombocytes as the preferred host cell type in buzzards. Thrombocytes
173 were clustered into four cellular subtypes. Whether these subtypes also display different functions and
174 host-parasite interactions remains to be investigated. Meanwhile, parasite transcripts were also
175 notably expressed at low levels in several host cell types indicating a probable widescale infection of
176 various non-preferred cell types. This global expression of parasite genes across host cell types under
177 HP might be due to a promiscuous invasion of host cells by merozoites under HP. The upregulation of

178 genes required for invasion of host cells by merozoites in *P. falciparum* such as *PfIMC1i* and *G2*
179 supports this interpretation[42]. We also observed an expression of different host cell-type markers in
180 different gametocyte subtypes, which might represent residual expression of host genes after invasion
181 or parasite-driven ectopic expression. Hence, parasite micro- and macrogametocytes might each
182 preferentially develop from different host peripheral blood cell types. In conclusion, our data suggests
183 thrombocytes as preferred host cell types of gametocytes, while low level expression of parasite
184 transcripts indicates a widescale invasion of host cell types under HP.

185 We found that host transcriptional profiles differed strongly between parasitaemia levels and in part
186 even displayed opposing trends comparing cells harbouring developing gametocytes, micro- and
187 macrogametocytes. Our findings indicate that developing versus differentiated gametocytes face and
188 in turn shape very different regulatory environments within their host cells. Firstly, the bulk of DEGs
189 occurred in developing gametocytes which indicates that transcriptional host-parasite antagonism
190 might peak during the onset of parasite development, when interactions are first calibrated and the
191 intracellular niche is established[43]. In fact, the reprogramming and restructuring of the host cell is well
192 known to require and elicit profound transcriptional changes by intracellular protozoa[44,45].

193 Secondly, we detected opposing patterns of differential expression in the different gametocyte
194 subtypes. This pattern was mainly observed for genes involved in host ribosome biogenesis, a process
195 which is also known to enhance growth and proliferation during carcinogenesis if deregulated[46]. While
196 these genes were downregulated under HP in developing gametocytes, they were upregulated in
197 microgametocytes. Meanwhile, no such pattern was observed in macrogametocytes. This could be
198 explained by an unknown density-dependent mechanism favouring host ribosome biogenesis in
199 developing gametocytes under low parasitaemia and in microgametocytes under high parasitaemia,
200 which would be absent in macrogametocytes. Beside downregulation of host genes encoding
201 ribosomal proteins in microgametocytes, we also observed downregulation of host RNA metabolism
202 possibly involved in re-allocation of resources towards parasitic gene expression along with a

203 deregulation of genes linked to the host's actin cytoskeleton also known to occur during the early
204 development of other intracellular protists[47–49].

205 A first important notion supporting the idea of immunosuppression during *L. toddi* infection was the
206 absence of pronounced differences in immune cell populations depending on the level of parasitaemia.
207 Many other intracellular parasites are known to prevent activation and clonal expansion of T cells and
208 other immune cells required for parasite clearance[12–14]. Second, the majority of differentially
209 expressed host genes were downregulated under HP. Concomitantly, we also found several genes
210 involved in the immune response to be downregulated under HP across multiple cell types. This
211 included downregulation of calgranulin- and avidin-encoding genes in CD4+ T cells or *NOS2* in
212 microgametocytes. In contrast to our observations, these genes have been shown to be
213 transcriptionally upregulated in response to LPS-injection in wild passerines and upon *Salmonella*
214 *enterica*-infection in chicken[50–52]. Another indication of immunosuppression was provided by the
215 downregulation of MHC-I and -II expression, which has been characterised as a mechanism of immune
216 evasion in *Leishmania donovani* and *Toxoplasma gondii* infection[53–56]. While a similar mechanism might
217 drive the downregulation of *B2M* in developing *L. toddi* gametocytes under HP, it remains puzzling that
218 we found the opposite effect in microgametocytes. On the other hand, a wide range of host cell types
219 also displayed upregulation of MHC-I components under HP. However, MHC-I upregulation did not
220 seem to evoke a strong CD8+ T cell response. This is suggested by a lack of a pronounced cytokine
221 response and downregulation of genes involved in CD8+ T cell activation. The weak and promiscuous
222 expression patterns of various cytokines indicate an overall mild inflammatory response regardless of
223 infection intensity. Additionally, this response is downregulated under HP in the case of *IL-8 like* and
224 *TGF-β* in thrombocytes. While the upregulation of *IL-8 like* under HP in eosinophils might contribute to
225 the inflammatory response, this effect might be neutralised by downregulation in thrombocytes. The
226 lack of differential expression of *IL-2, IL-16, IL-18, IL-7*, *IL-15, TNF11*, *TNF13B* and *TNF8 like* comparing
227 between LP and HP does not indicate a correlation with parasitaemia. The expression of these genes
228 might either be constitutive or induced during the onset of infection without further increase during

229 the course of infection. Finally, the expression of immunoglobulins remained stable or was even
230 downregulated under HP, which is also in agreement with the finding that antibody titres of buzzard
231 nestlings could not be linked to *Leucocytozoon* infection intensity in an earlier study by our group[57].

232 The widescale downregulation of several immune genes could indicate the presence of
233 immunosuppressive effects under high *Leucocytozoon* infection intensity. As this pattern can result
234 from the inter-individual variation of host immunity and infection trajectories it would need to be
235 addressed by performing experimental infections. However, such experiments are both logistically and
236 ethically unfeasible with *Leucocytozoon* in protected free-living raptor hosts. For this purpose, other
237 comparable models would need to be developed. Thus, while we cannot be secure that widescale
238 downregulation of immune genes is the outcome of manipulation by the parasite, this interpretation
239 seems likely.

240 Within the various peripheral blood cell-types we observed highly cell-type specific transcriptional
241 responses to parasitaemia, some of which might be reactions to manipulation by the parasite. A vast
242 body of literature on comparable host-parasite systems suggests the functions of genes which exhibit
243 parasitaemia-related expression changes. Although these connections remain speculative, they can
244 help to understand how and which mechanisms utilised by other intracellular protozoa for host
245 manipulation might be at play in *Leucocytozoon*.

246 Overall, we observed a repetitive pattern of cell-type specific downregulation of immune genes in
247 various host cell types. On the other hand, certain genes could confer tolerance to infection. Other
248 genes were implicated in promoting parasite growth.

249 An example of cell-type specific downregulation of immune genes could be provided by the
250 downregulation of *DTNA* and of *CCDC155* in CD4+ T cells potentially affecting T cell activation. DTNA is
251 known as a component of the DGC (dystrophin-glycoprotein complex) found in striated muscle cells[58].
252 CCDC155 has been characterised as a component of the LINC (linkers of the nucleoskeleton to the
253 cytoskeleton)-complex coupling chromosomes to the cytoskeleton during meiosis[59]. Interestingly,

254 immunological synapse formation during T cell activation involves both the LINC-complex and the
255 DGC[60,61].

256 T cell activation might also be suppressed in CD8+ T cells, since some genes known to be involved in
257 this process were downregulated under HP. For instance, *TXNRD1* is upregulated during activation and
258 clonal expansion of T cells in response to *Leishmania major* infection[62]. Consequently, *TXNRD1*-
259 deficiency leads to increased parasitaemia[62].

260 In microgametocytes the downregulation of *NOS2* under HP might play a role in increasing host
261 tolerance to infection. Intracellular protists are known to downregulate iNOS as a mechanism of
262 immune evasion as exemplified by *T. gondii* and *L. amazonensis* infections[63,64]. Inducible nitric oxide
263 synthase (iNOS) encoded by *NOS2* catalyses the production of anti-parasitic nitric oxide (NO), which at
264 excess causes cytotoxic damage to the host[65–67]. Therefore, a downregulation of *NOS2* might be
265 beneficial, especially under high parasite burden and highlights the possibility of a mechanism enabling
266 tolerance to infection.

267 As an example of a gene potentially promoting parasite growth, *FTH1,* encoding a subunit of ferritin
268 required for iron homeostasis was upregulated under HP in thrombocytes. Ferritin confers tolerance
269 to malaria in humans[68]. However, this is unlikely to be the case during *Leucocytozoon*-infections since
270 they do not cause haemolysis and excessive release of iron as seen in *Plasmodium*-infections[18]. A
271 mechanism as observed in *Leishmania amazonensis*-infected macrophages is more likely, where FTH1
272 promotes parasite growth through iron scavenging[69]. This interpretation is further supported by the
273 notion that *FTH1* was also upregulated in microgametocytes.

274 Our findings indicate that the low virulence of *L. toddi* is associated with widescale downregulation of
275 immune genes in peripheral blood. At the same time, the sampled individuals might differ in their
276 susceptibility to infection or represent different time points of infection, which may also correspond
277 to different immunological responses. Immunosuppression can prevent excessive immune responses,
278 which can be damaging to the host (e. g. excessive cytokine production[45]). Therefore, the inhibition of

such pathways during parasitic infections can be beneficial to the host under certain circumstances such as low parasite virulence. For instance, costs of infection may be resource-dependent and thus could be compensated by additional food provisioning as long as buzzard nestlings are provided with parental care[22]. Accordingly, current work by our group shows that *Leucocytozoon* infection at the nestling stage is not predictive of survival (Ottensmann et al., in press). Immune evasion can have a mitigating effect on virulence and in certain contexts assist the evolution of host tolerance[3]. In this light, our study provides a rare example of reduced immunopathology in an apparently highly co-adapted host-parasite-system elucidated down to the cellular and molecular mechanisms. It therefore contributes a rarely detailed reference within a spectrum of strategies and levels of host-parasite antagonism that still remains to be understood in the wild nature.

289 # Methods

290 **Sample acquisition and preparation**

291 Samples were collected in June 2021 in a population of Common Buzzards in eastern Westphalia,
292 Germany (8°25'E and 52°06'N). Occupied nests had previously been located in March and April. In a
293 first sampling event, blood samples were taken from the ulnar vein of nestlings. Air-dried blood smears
294 were prepared in the field, fixed in absolute ethanol and stained with Giemsa[18]. Parasitaemia of *L.*
295 *toddi* was estimated microscopically based on gametocyte counts. From this pool of sampled 345
296 buzzard nestlings from 164 territories, six individuals were chosen for further sampling based on their
297 infection status ("low" versus "high" parasitaemia; Tab. S1). Uninfected nestlings were not available
298 due to the extremely high prevalence of the parasite in the study population. Selected individuals
299 originated from six different breeding territories, which were evenly distributed throughout the study
300 area. In a second sampling event (maximum ten days after first sampling), three individuals with "low
301 parasitaemia" (LP: 0.017%, 0.025% & 0.133% of total blood cells) and three individuals with "high
302 parasitaemia" (HP: 0.956%, 1.384% & 1.699% of total blood cells) were brought to the Genomics &
303 Transcriptomics Laboratory of the Heinrich-Heine-University in Düsseldorf, Germany. A blood sample
304 with a volume of 1 mL was taken from the ulnar vein, transferred to a 15 mL centrifuge tube for Percoll
305 (Sigma-Aldrich) density gradient centrifugation with discontinuous layers of 55%, 45%, 35%, and 25%
306 solutions of stock isotonic Percoll (SIP) diluted with PBS at 7.4 pH. The density gradient centrifugation
307 was performed to deplete erythrocytes (swinging-bucket centrifuge rotor, 500 x g, 15min at 20°C). The
308 easily visible upper non-erythrocytic phases, containing larger and less dense cells compared to avian
309 erythrocytes, were extracted, and immediately subjected to single cell processing. Variation in the
310 extraction of leukocytes may cause differences in cell type proportions between samples. For
311 comparison of cell type proportions with scRNA-seq all peripheral blood cell types were counted via
312 microscopy of blood smears. Per sample approximately 30000 cells were counted within 20 random
313 fields of view (Tab. S2). The nestlings were immediately returned to their nests after sampling and
314 transport. Sampling and transport of nestlings were permitted by the ethics commission of the Animal

315 Care and Use Committee of the German North Rhine-Westphalia State Office for Nature, Environment
316 and Consumer Protection (Landesamt für Natur, Umwelt und Verbraucherschutz Nordrhein-
317 Westfalen) under the reference number 84-02.04.2017.A147.

318 **Single Cell Library Generation**

319 A total of ~40,000 single cells were generated on the 10X Chromium Controller system for single-cell
320 droplet library generation utilizing the Chromium Single Cell 3' NextGEM Reagent Kit v3.1 (10X
321 Genomics, Pleasanton, CA, USA) according to manufacturer's instructions. Sequencing was carried out
322 on a NextSeq550 system (Illumina Inc. San Diego, USA) with a mean sequencing depth of ~50,000
323 reads/cell.

324 **Processing of 10X Genomics single cell data**

325 Raw sequencing data were processed using the 10X Genomics CellRanger software (v7.0). Raw BCL-
326 files were demultipexed and processed to Fastq-files using the CellRanger *mkfastq* pipeline. A custom
327 reference was created by combining draft *B. buteo* and *L. toddi* genomes using the cellranger *mkref*
328 pipeline. Alignment of reads to the genome and UMI (unique molecular identifier) counting was
329 performed via the CellRanger *count* pipeline to generate a gene-barcode matrix. All samples were
330 aggregated and normalised for sequencing depth using the cellranger *aggr* pipeline.

331 Further analyses were carried out with the Seurat v4.1.1 R package[70–72]. Initial quality control consisted
332 of removal of cells with fewer than 200 detected genes as well as removal of genes expressed in less
333 than three cells. Furthermore, cells with a mapping rate of > 10% to the mitochondrial genome were
334 removed, as they most likely represent dead or damaged cells. Cell doublets were removed from the
335 dataset using DoubletFinder v2.0[73]. Normalization was carried out utilizing SCTransform. Dimensional
336 reduction of the data set was achieved by Principal Component analysis (PCA), based on identified
337 variable genes and subsequent UMAP (Uniform Manifold Approximation and Projection) embedding.
338 The number of meaningful Principal Components (PC) was selected by ranking them according to the
339 percentage of variance explained by each PC, plotting them in an "Elbow Plot" and manually

340 determining the number of PCs that represent the majority of variance in the data set. Cells were
341 clustered using the graph-based clustering approach implemented in Seurat. Marker genes defining
342 each cluster (MGs) as well as differentially expressed genes (DEGs) comparing LP and HP nestlings were
343 calculated using a Wilcoxon Rank Sum test implemented in Seurat. Additionally, correlated gene
344 expression with parasitaemia determined by blood smear cell counts (see methods above) were
345 performed. Linear models were fitted to the averaged expression of each gene per cluster versus the
346 gradient of parasitaemia values to identify correlated genes (CGs). The false discovery rate was
347 calculated to account for multiple testing.

348 **Cluster annotation and downstream analyses**

349 Literature-curated markers were used to annotate Seurat clusters with avian peripheral blood cell
350 types and haemosporidian gametocyte stages (Fig. 1, S3 & S4). Blood cell markers from *Gallus gallus*
351 and *Plasmodium falciparum* (lineage 3D7) gametocyte markers were utilised[33,74–79]. The annotation of
352 cell types was further aided by the overall similarity of transcriptional profiles (Fig. 1A), marker genes
353 with indicative functions (MGs; Tab. S3) and parasite transcript abundance (Fig. S1D, Fig. S2). Multiple
354 clusters could be grouped into one cell type based on the expression of marker genes, while the
355 identity of subtypes remained elusive. Downstream analyses were performed using R version 4.1.2 for
356 data processing and exploration[80].

357 **Network analysis of DEGs**

358 Protein-protein-interaction (PPI) network analysis of host DEGs was conducted with Cytoscape
359 stringApp v2 using *Aquila chrysaetos chrysaetos* as reference species to generate networks based on
360 DEGs with cut-off values $p \geq 0.05$ (Bonferroni adjusted) and $\log_2$FC (averaged per cluster) ≥ 1[81–83]. Only
361 interactions with a confidence score of ≥ 0.9 were retrieved. Pathway enrichment analysis was
362 performed via the enrichment tool implemented in stringApp v2 using the referenced genome as a
363 background. For comparability, only enriched KEGG (Kyoto Encyclopedia of Genes and Genomes)
364 pathways were highlighted.

Data and resource availability

The .fastq-files containing scRNA-seq sequences are deposited in the European Nucleotide Archive (ENA) at EMBL-EBI under accession number PRJEB73843. R-code for downstream analyses is accessible via Dryad (DOI: 10.5061/dryad.sbcc2frf2).

Acknowledgments

Sampling and processing of the samples was supported by the German Research Foundation (DFG), as part of the SFB TRR 212 (NC^3) – project numbers 316099922 and 396780709 and DFG project number 398434413 to OK and NC. This work was supported by the DFG Research Infrastructure West German Genome Center, project 407493903, as part of the Next Generation Sequencing Competence Network, project 423957469. Next Generation Sequencingand/or analyses was carried out at the West German Genome Center Düsseldorf. NC and OK received the DFG grant #DJ 154/4-4 as part of the DFG Sequencing call #2. Computational infrastructure and support were provided by the Centre for Information and Media Technology at Heinrich Heine University Düsseldorf and from the Center for Biotechnology, CeBiTec, Bielefeld University.

Author contributions

NC and OK designed the research. NC was involved in sample acquisition. NC and TL performed laboratory procedures. TL and TMR analysed the data. TMR wrote the paper. RP and JK provided critical feedback to the analyses and the manuscript.

383 # Tables and Figures

384 Table 1: Strongest DEGs across clusters (ordered by cell type). References indicate potential gene
385 functions. Immune genes upregulated under HP are indicated by "↑", whereas immunosuppression
386 (downregulation of immune genes under HP) is indicated by "↓" (see column "Function"). Reference
387 (Ref.) species: Ac = *Aquila chrysaetos chrysaetos*, Cm = *Corvus moneduloides*, Gg = *Gallus gallus*, Pm =
388 *Parus major*, Pf = *Plasmodium falciparum 3D7*, Bb = *Babesia bigemina.*

Cluster	Para-sitemia	NCBI accession number	Gene	Ref. species	log_2-FC (avg.)	p-value (adj.)	Function	References
			Host					
9	HP	XP_031958267.1	*PHF10*	*Cm*	-1.36	1.65E-09	chromatin remodelling	84
	LP	XP_031970858.1	*TSSK6*	*Cm*	1.00	6.51E-06	chromatin remodelling	85
	LP	XP_040977087.1	*LOC121232750*	*Ac*	1.23	6.40E-06	-	-
	LP	XP_015480400.1	*MXD4*	*Pm*	1.86	5.18E-07	↓ blood progenitor proliferation, T cell survival	86,87
	LP	XP_029888348.1	*CDC42BPB*	*Ac*	2.14	6.93E-05	regulator of the cytoskeleton	88
0	HP	XP_029862693.1	*LOC115338306*	*Ac*	-1.11	4.05E-71	↑ MHC-I	89
	LP	XP_029877109.1	*ESAM*	*Ac*	1.49	1.16E-130	↓ neutrophil extravasation	90,91
1	HP	XP_029851964.1	*SYN2*	*Ac*	-2.03	2.68E-108	exocytosis	92–94
	LP	XP_040547522.1	*EYA1*	*Gg*	1.12	1.21E-68	DNA repair	95–97
	LP	XP_029877109.1	*ESAM*	*Ac*	1.41	1.11E-129	↓ neutrophil extravasation	90,91
3	HP	XP_029851964.1	*SYN2*	*Ac*	-2.14	5.52E-84	exocytosis	92–94
	HP	XP_029895765.1	*FTH1*	*Ac*	-1.01	1.17E-02	iron scavenging	68,69
	LP	XP_029859213.1	*MTMR12*	*Ac*	1.05	2.72E-21	endocytosis	98–100
	LP	XP_029852971.2	*ARHGAP36*	*Ac*	1.11	1.50E-51	neural development	101–103
	LP	XP_040547522.1	*EYA1*	*Gg*	1.16	2.01E-26	DNA repair	95–97
7	HP	XP_029851964.1	*SYN2*	*Ac*	-2.13	2.19E-81	exocytosis	92–94
	HP	XP_029866592.1	*PPDPF*	*Ac*	-1.29	5.16E-23	implicated in cancer progression	104,105
	LP	XP_029852971.2	*ARHGAP36*	*Ac*	1.10	1.28E-44	neural development	101–103
2	LP	XP_031953757.1	*CCDC155*	*Cm*	1.23	2.88E-89	↓ T cell activation	59,60
	LP	XP_018861179.1	*DTNA*	*Pm*	1.68	6.03E-162	↓ T cell activation	58,61
5	LP	XP_018861179.1	*DTNA*	*Pm*	1.04	8.17E-69	↓ T cell activation	58,61
8	LP	XP_018861179.1	*DTNA*	*Pm*	1.29	9.21E-67	↓ T cell activation	58,61
11	LP	XP_031953757.1	*CCDC155*	*Cm*	1.23	3.95E-17	↓ T cell activation	59,60
	LP	XP_018861179.1	*DTNA*	*Pm*	1.93	1.84E-40	↓ T cell activation	58,61
16	LP	XP_029861532.1	*LOC115337405*	*Ac*	1.32	7.03E-06	↓ anti-pathogenic	106
	LP	XP_029879656.2	*LOC115345306*	*Ac*	1.45	1.68E-04	↓ pro-inflammatory	107
18	LP	XP_029896238.1	*TXNRD1*	*Ac*	1.62	2.97E-11	↓ T cell activation	62
	LP	XP_029886923.1	*ALOX5*	*Ac*	1.63	3.08E-10	↓ T cell activation, inflammation & cell death	108–110
	LP	XP_018861179.1	*DTNA*	*Pm*	1.68	1.79E-08	↓ T cell activation	58,61
19	LP	XP_040977722.1	*LOC115337909*	*Ac*	1.01	1.04E-07	↓ T cell activation (putative)	111
	LP	XP_018861179.1	*DTNA*	*Pm*	1.02	1.57E-05	↓ T cell activation	58,61
	LP	XP_031953757.1	*CCDC155*	*Cm*	1.11	3.28E-05	↓ T cell activation	59,60
10	LP	XP_029881352.1	*S100A10*	*Ac*	1.44	1.25E-16	↓ pro-inflammatory	112
12	HP	XP_040977087.1	*LOC121232750*	*Ac*	-1.05	2.52E-44	-	-
	LP	XP_029862549.1	*LOC115338209*	*Ac*	1.19	6.80E-65	↓ MHC-II	55,56
4	HP	XP_029897790.1	*F13A1*	*Ac*	-1.19	3.19E-25	coagulation factor	113
	LP	XP_029861378.1	*ANXA1*	*Ac*	1.11	2.52E-27	↓ neutrophil extravasation	114
	LP	XP_029879656.2	*LOC115345306*	*Ac*	2.90	3.09E-48	↓ pro-inflammatory	107
13	HP	XP_040978593.1	*CSRNP1*	*Ac*	-1.05	7.52E-16	↑ immune cell growth & development	115
	LP	XP_029897792.1	*LY86*	*Ac*	1.03	1.33E-10	↓ regulator of Toll-Signalling	116
15	LP	XP_029871069.1	*LOC115341780*	*Ac*	2.71	9.06E-07	↓ anti-pathogenic (putative)	117
20	HP	XP_029893214.2	*FAM184A*	*Ac*	-1.39	6.19E-03	associated with human malignancies	118–120
6	HP	XP_029895765.1	*FTH1*	*Ac*	-2.67	1.90E-13	iron scavenging	68,69
	HP	XP_029893758.1	*LOC115351288*	*Ac*	-2.30	6.81E-08	antioxidant	121
	HP	XP_040977744.1	*LOC121233102*	*Ac*	-2.02	3.62E-09	carcinogenesis (putative)	122
	HP	XP_031957654.1	*RPS12*	*Cm*	-1.98	2.18E-09	ribosome	46
	HP	XP_029860305.1	*EMC4*	*Ac*	-1.89	6.82E-08	protein folding	123,124
	LP	XP_029890446.1	*LOC115349840*	*Ac*	3.88	3.78E-04	↓ anti-pathogenic (putative)	125–127
	LP	XP_029863942.1	*XRCC2*	*Ac*	4.01	1.84E-22	DNA repair	128,129
	LP	XP_029856482.1	*BTG2*	*Ac*	4.28	1.15E-13	↓ pleiotropic tumour suppressor gene	130,131
	LP	XP_029883424.1	*NOS2*	*Ac*	5.76	6.91E-26	↓ anti-pathogenic	65–67
	LP	XP_029871871.1	*PRKCQ*	*Ac*	6.47	8.03E-178	↓ T cell & platelet activation	132
17	LP	XP_029854753.1	*PRKD1*	*Ac*	3.95	5.47E-29	↓ T cell activation, pro-inflammatory	133,134
	LP	XP_040980327.1	*ARHGAP15*	*Ac*	4.09	1.57E-06	regulator of the cytoskeleton	135
	LP	XP_029883957.1	*VEZF1*	*Ac*	4.25	3.79E-21	↓ septic shock	136,137
	LP	XP_029863942.1	*XRCC2*	*Ac*	4.62	1.63E-19	DNA repair	128,129
	LP	XP_029888348.1	*CDC42BPB*	*Ac*	4.84	1.63E-24	regulator of the cytoskeleton	88
			Parasite					
9	HP	XP_024329154.1	*PF3D7_1214500*	*Pf*	-3.20	1.34E-51	enriched in gametocytes	138
	HP	XP_002585477.1	*PF3D7_1466500*	*Pf*	-2.93	1.04E-32	-	-
	HP	XP_002809016.1	*PF3D7_1316300*	*Pf*	-2.81	2.06E-33	-	-
	HP	XP_001349289.1	*PfIMC1i (PF3D7_0823500)*	*Pf*	-2.75	2.72E-36	morphological changes	42
	HP	XP_001350486.1	*Pf41-3 precursor (PF3D7_1207700)*	*Pf*	-2.58	1.53E-23	enriched in gametocytes	138

Cluster	Para-sitemia	NCBI accession number	Gene	Ref. species	log_2-FC (avg.)	p-value (adj.)	Function	References
0	HP	XP_001349289.1	*PfIMC1i (PF3D7_0823500)*	*Pf*	-4.02	0.00E+00	morphological changes	42
	HP	XP_024329154.1	*PF3D7_1214500*	*Pf*	-3.94	0.00E+00	enriched in gametocytes	138
	HP	XP_002809016.1	*PF3D7_1316300*	*Pf*	-3.47	0.00E+00	-	-
	HP	XP_001348354.1	*PfPLC6 (PF3D7_1418300)*	*Pf*	-3.36	0.00E+00	host cell invasion (putative)	139,140
	HP	XP_002585477.1	*PF3D7_1466500*	*Pf*	-3.28	0.00E+00	-	-
1	HP	XP_001349289.1	*PfIMC1i (PF3D7_0823500)*	*Pf*	-4.09	0.00E+00	morphological changes	42
	HP	XP_024329154.1	*PF3D7_1214500*	*Pf*	-3.90	0.00E+00	enriched in gametocytes	138
	HP	XP_002809016.1	*PF3D7_1316300*	*Pf*	-3.39	0.00E+00	-	-
	HP	XP_001348354.1	*PfPLC6 (PF3D7_1418300)*	*Pf*	-3.29	0.00E+00	host cell invasion (putative)	139,140
	HP	XP_002808700.1	*PfPSOP13 (PF3D7_0518800)*	*Pf*	-3.21	0.00E+00	host-to-vector transmission	141
3	HP	XP_001349289.1	*PfIMC1i (PF3D7_0823500)*	*Pf*	-4.19	0.00E+00	morphological changes	42
	HP	XP_024329154.1	*PF3D7_1214500*	*Pf*	-4.10	0.00E+00	enriched in gametocytes	138
	HP	XP_002809016.1	*PF3D7_1316300*	*Pf*	-3.53	0.00E+00	-	-
	HP	XP_001352166.1	*PF3D7_0929600*	*Pf*	-3.52	3.41E-294	morphological changes (putative)	42
	HP	XP_001348354.1	*PfPLC6 (PF3D7_1418300)*	*Pf*	-3.51	1.17E-281	host cell invasion (putative)	139,140
7	HP	XP_001349289.1	*PfIMC1i (PF3D7_0823500)*	*Pf*	-3.93	1.33E-231	morphological changes	42
	HP	XP_024329154.1	*PF3D7_1214500*	*Pf*	-3.77	1.32E-260	enriched in gametocytes	138
	HP	XP_002585477.1	*PF3D7_1466500*	*Pf*	-3.12	5.77E-159	-	-
	HP	XP_002809016.1	*PF3D7_1316300*	*Pf*	-3.10	1.10E-170	-	-
	HP	XP_001348354.1	*PfPLC6 (PF3D7_1418300)*	*Pf*	-3.06	2.76E-145	host cell invasion (putative)	139,140
2	HP	XP_024329154.1	*PF3D7_1214500*	*Pf*	-2.73	0.00E+00	enriched in gametocytes	138
	HP	XP_001349289.1	*PfIMC1i (PF3D7_0823500)*	*Pf*	-2.22	0.00E+00	morphological changes	42
	HP	XP_002809016.1	*PF3D7_1316300*	*Pf*	-2.08	0.00E+00	-	-
	HP	XP_001352166.1	*PF3D7_0929600*	*Pf*	-1.90	1.09E-296	morphological changes (putative)	42
	HP	XP_002585477.1	*PF3D7_1466500*	*Pf*	-1.89	3.03E-265	-	-
5	HP	XP_024329154.1	*PF3D7_1214500*	*Pf*	-2.39	0.00E+00	enriched in gametocytes	138
	HP	XP_001349289.1	*PfIMC1i (PF3D7_0823500)*	*Pf*	-1.81	1.88E-269	morphological changes	42
	HP	XP_002809016.1	*PF3D7_1316300*	*Pf*	-1.71	1.89E-255	-	-
	HP	XP_002585477.1	*PF3D7_1466500*	*Pf*	-1.67	2.83E-243	-	-
	HP	XP_001352166.1	*PF3D7_0929600*	*Pf*	-1.62	9.67E-253	morphological changes (putative)	42
8	HP	XP_024329154.1	*PF3D7_1214500*	*Pf*	-2.21	1.52E-263	enriched in gametocytes	138
	HP	XP_001349289.1	*PfIMC1i (PF3D7_0823500)*	*Pf*	-1.71	2.97E-189	morphological changes	42
	HP	XP_002809016.1	*PF3D7_1316300*	*Pf*	-1.51	1.26E-191	-	-
	HP	XP_001352166.1	*PF3D7_0929600*	*Pf*	-1.46	8.34E-183	morphological changes (putative)	42
	HP	XP_002585477.1	*PF3D7_1466500*	*Pf*	-1.34	1.26E-170	-	-
11	HP	XP_024329154.1	*PF3D7_1214500*	*Pf*	-4.12	2.69E-164	enriched in gametocytes	138
	HP	XP_001349289.1	*PfIMC1i (PF3D7_0823500)*	*Pf*	-3.63	1.19E-131	morphological changes	42
	HP	XP_002809016.1	*PF3D7_1316300*	*Pf*	-3.28	3.98E-107	-	-
	HP	XP_002585477.1	*PF3D7_1466500*	*Pf*	-3.20	1.04E-105	-	-
	HP	XP_002808700.1	*PfPSOP13 (PF3D7_0518800)*	*Pf*	-2.98	7.70E-101	host-to-vector transmission	141
16	HP	XP_024329154.1	*PF3D7_1214500*	*Pf*	-1.90	8.40E-78	enriched in gametocytes	138
	HP	XP_001349289.1	*PfIMC1i (PF3D7_0823500)*	*Pf*	-1.38	6.61E-50	morphological changes	42
	HP	XP_001348354.1	*PfPLC6 (PF3D7_1418300)*	*Pf*	-1.28	8.83E-66	host cell invasion (putative)	139,140
	HP	XP_002809016.1	*PF3D7_1316300*	*Pf*	-1.24	1.64E-63	-	-
	HP	XP_001352166.1	*PF3D7_0929600*	*Pf*	-1.15	1.11E-54	morphological changes (putative)	42
18	HP	XP_024329154.1	*PF3D7_1214500*	*Pf*	-3.09	1.80E-50	enriched in gametocytes	138
	HP	XP_001349289.1	*PfIMC1i (PF3D7_0823500)*	*Pf*	-2.55	3.51E-36	morphological changes	42
	HP	XP_002809016.1	*PF3D7_1316300*	*Pf*	-2.18	4.20E-37	-	-
	HP	XP_002585477.1	*PF3D7_1466500*	*Pf*	-2.16	3.52E-31	-	-
	HP	XP_001352166.1	*PF3D7_0929600*	*Pf*	-2.13	1.44E-37	morphological changes (putative)	42
19	HP	XP_001350425.1	*PfNEK3 (PF3D7_1201600)*	*Pf*	-2.11	5.74E-07	cell cycle regulation	142
	HP	XP_024329154.1	*PF3D7_1214500*	*Pf*	-2.09	9.48E-36	enriched in gametocytes	138
	HP	XP_001349289.1	*PfIMC1i (PF3D7_0823500)*	*Pf*	-1.54	4.42E-20	morphological changes	42
	HP	XP_002809016.1	*PF3D7_1316300*	*Pf*	-1.50	1.24E-27	-	-
	HP	XP_002585477.1	*PF3D7_1466500*	*Pf*	-1.36	2.19E-22	-	-
10	HP	XP_024329154.1	*PF3D7_1214500*	*Pf*	-2.90	8.26E-171	enriched in gametocytes	138
	HP	XP_002809016.1	*PF3D7_1316300*	*Pf*	-2.68	4.27E-128	-	-
	HP	XP_001350486.1	*Pf41-3 precursor (PF3D7_1207700)*	*Pf*	-2.60	1.04E-90	enriched in gametocytes	138
	HP	XP_001350425.1	*PfNEK3 (PF3D7_1201600)*	*Pf*	-2.54	1.50E-48	cell cycle regulation	142
	HP	XP_002585477.1	*PF3D7_1466500*	*Pf*	-2.43	6.87E-96	-	-
12	HP	XP_024329154.1	*PF3D7_1214500*	*Pf*	-2.05	8.31E-127	enriched in gametocytes	138
	HP	XP_001350486.1	*Pf41-3 precursor (PF3D7_1207700)*	*Pf*	-1.96	7.91E-58	enriched in gametocytes	138
	HP	XP_002585477.1	*PF3D7_1466500*	*Pf*	-1.82	3.86E-71	-	-
	HP	XP_002809016.1	*PF3D7_1316300*	*Pf*	-1.80	1.66E-79	-	-
	HP	XP_001352166.1	*PF3D7_0929600*	*Pf*	-1.69	1.99E-96	morphological changes (putative)	42
21	HP	XP_024329154.1	*PF3D7_1214500*	*Pf*	-1.27	2.40E-11	enriched in gametocytes	138
4	HP	XP_024329154.1	*PF3D7_1214500*	*Pf*	-4.05	0.00E+00	enriched in gametocytes	138
	HP	XP_002809016.1	*PF3D7_1316300*	*Pf*	-3.45	0.00E+00	-	-

Cluster	Para-sitemia	NCBI accession number	Gene	Ref. species	log_2-FC (avg.)	p-value (adj.)	Function	References
	HP	XP_001349289.1	*PfIMC1i (PF3D7_0823500)*	*Pf*	-3.43	0.00E+00	morphological changes	[42]
	HP	XP_002585477.1	*PF3D7_1466500*	*Pf*	-3.25	0.00E+00	-	-
	HP	XP_001352166.1	*PF3D7_0929600*	*Pf*	-3.24	0.00E+00	morphological changes (putative)	[42]
13	HP	XP_024329154.1	*PF3D7_1214500*	*Pf*	-2.63	1.65E-133	enriched in gametocytes	[138]
	HP	XP_001349289.1	*PfIMC1i (PF3D7_0823500)*	*Pf*	-2.26	3.82E-111	morphological changes	[42]
	HP	XP_002809016.1	*PF3D7_1316300*	*Pf*	-2.18	1.17E-95	-	-
	HP	XP_002585477.1	*PF3D7_1466500*	*Pf*	-2.07	1.95E-88	-	-
	HP	XP_001352166.1	*PF3D7_0929600*	*Pf*	-2.04	4.98E-88	morphological changes (putative)	[42]
15	HP	XP_024329154.1	*PF3D7_1214500*	*Pf*	-3.15	5.74E-64	enriched in gametocytes	[138]
	HP	XP_001350486.1	*Pf41-3 precursor (PF3D7_1207700)*	*Pf*	-2.94	1.84E-35	enriched in gametocytes	[138]
	HP	XP_002809016.1	*PF3D7_1316300*	*Pf*	-2.85	1.00E-41	-	-
	HP	XP_002585477.1	*PF3D7_1466500*	*Pf*	-2.67	6.10E-41	-	-
	HP	XP_001352166.1	*PF3D7_0929600*	*Pf*	-2.53	2.39E-56	morphological changes (putative)	[42]
20	HP	XP_002809016.1	*PF3D7_1316300*	*Pf*	-3.04	5.49E-18	-	-
	HP	XP_001349289.1	*PfIMC1i (PF3D7_0823500)*	*Pf*	-3.01	8.78E-19	morphological changes	[42]
	HP	XP_024329154.1	*PF3D7_1214500*	*Pf*	-2.94	1.38E-19	enriched in gametocytes	[138]
	HP	XP_001352166.1	*PF3D7_0929600*	*Pf*	-2.80	1.01E-17	morphological changes (putative)	[42]
	HP	XP_001348354.1	*PfPLC6 (PF3D7_1418300)*	*Pf*	-2.67	6.73E-17	host cell invasion (putative)	[139,140]
6	HP	XP_012769598.1	*BBBOND_0313150*	*Bb*	-2.91	5.00E-13	ABC-transporter	[143]
	HP	XP_001348212.1	*PF3D7_1404200*	*Pf*	-2.75	1.11E-12	-	-
	HP	XP_001349319.1	*PF3D7_0820600*	*Pf*	-2.63	2.72E-12	apicoplast (putative)	[144]
	HP	XP_001348354.1	*PfPLC6 (PF3D7_1418300)*	*Pf*	-2.56	7.22E-10	host cell invasion (putative)	[139,140]
	HP	XP_001348121.1	*PfRPS21 (PF3D7_1144000)*	*Pf*	-2.46	1.03E-09	ribosome	[145]
	LP	XP_001349989.1	*PfLDH (PF3D7_1324900)*	*Pf*	2.46	5.45E-10	lactic acid fermentation	[146,147]
	LP	XP_001347965.1	*PfPFK11 (PF3D7_1128300)*	*Pf*	2.88	2.15E-44	enriched in gametocytes	[148]
	LP	XP_001351121.1	*PfGLP1 (PF3D7_0304500)*	*Pf*	3.31	3.56E-12	glutaredoxin	[149]
14	LP	XP_002585462.1	*PfRPA3 (PF3D7_1442100)*	*Pf*	1.70	6.96E-03	DNA repair	[150]
	LP	XP_001350447.1	*PfUBC (PF3D7_1203900)*	*Pf*	2.30	1.02E-03	protein degradation	[151]
17	HP	XP_001350425.1	*PfNEK3 (PF3D7_1201600)*	*Pf*	-6.49	1.25E-29	cell cycle regulation	[142]
	HP	XP_001349778.1	*PfApiAP2 (PF3D7_1305200)*	*Pf*	-5.43	2.50E-23	repressed in macrogametocytes	[38]
	HP	XP_001349787.1	*PF3D7_1306000*	*Pf*	-5.00	2.24E-14	-	-
	HP	XP_966163.1	*PfH2A (PF3D7_0617800)*	*Pf*	-4.76	9.46E-34	histone protein	[152]
	HP	XP_002808835.1	*PfPPM5 (PF3D7_0810300)*	*Pf*	-4.71	5.84E-27	oocyst development	[153]

389

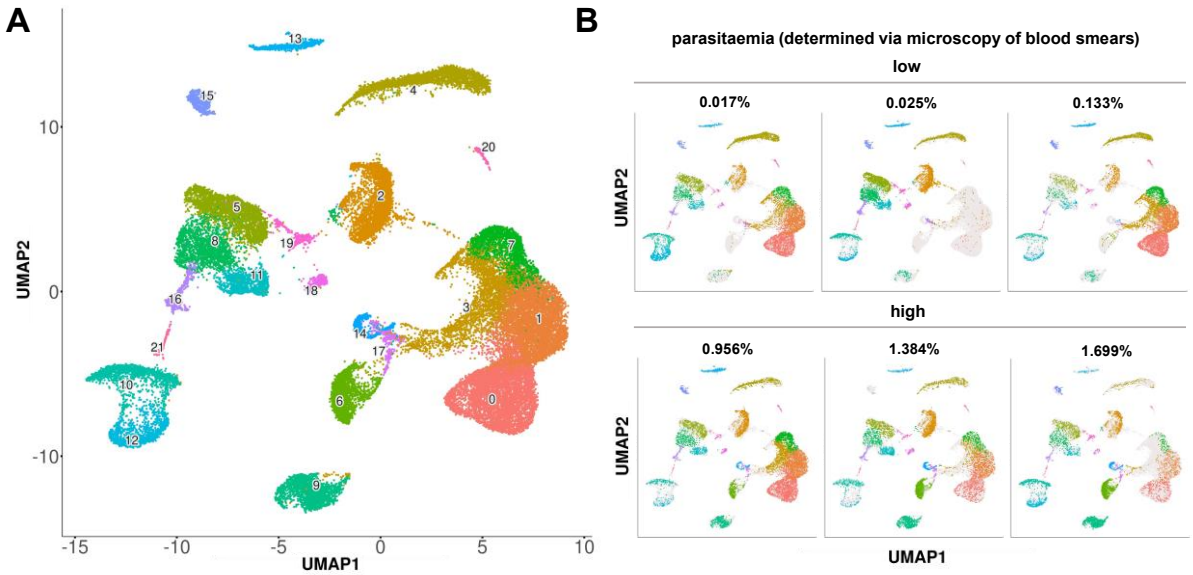

C

	cluster	annotation	total relative abundance	parasitaemia (via blood smears) 0.017%	0.025%	0.133%	0.956%	1.384%	1.699%
				relative abundance per sample					
host	9	erythrocytes	0.049	0.005	0.016	0.012	0.046	0.100	0.141
host	0	thrombocytes	0.145	0.195	0.004	0.255	0.184	0.094	0.072
host	1		0.136	0.182	0.005	0.208	0.182	0.109	0.069
host	3		0.080	0.094	0.013	0.144	0.120	0.049	0.016
host	7		0.052	0.054	0.000	0.078	0.086	0.046	0.019
host	2	CD4+T cells	0.084	0.044	0.205	0.037	0.067	0.108	0.074
host	5		0.068	0.058	0.181	0.023	0.047	0.061	0.064
host	8		0.049	0.038	0.129	0.015	0.036	0.047	0.050
host	11		0.032	0.020	0.069	0.012	0.023	0.054	0.022
host	16		0.014	0.010	0.037	0.005	0.010	0.017	0.009
host	18	CD8+T cells	0.009	0.003	0.028	0.002	0.008	0.013	0.005
host	19		0.009	0.005	0.024	0.005	0.004	0.007	0.013
host	10	B cells	0.040	0.044	0.071	0.022	0.019	0.035	0.071
host	12		0.029	0.063	0.036	0.018	0.010	0.008	0.050
host	21		0.003	0.003	0.004	0.002	0.001	0.003	0.005
host	4	putative heterophils	0.078	0.146	0.097	0.093	0.050	0.052	0.017
host	13	putative eosinophils	0.026	0.013	0.050	0.029	0.037	0.014	0.010
host	15	putative monocytes	0.014	0.009	0.022	0.017	0.015	0.001	0.023
host	20	unannotated	0.005	0.006	0.002	0.014	0.005	0.002	0.001
parasite	6	putative microgametocytes	0.053	0.001	0.000	0.004	0.033	0.130	0.188
parasite	14	putative macrogametocytes	0.016	0.000	0.000	0.003	0.011	0.037	0.055
parasite	17	putative developing gametocytes	0.010	0.007	0.008	0.004	0.007	0.013	0.025

Figure 1: Overview of scRNA-seq clusters (Seurat clusters) and their proportions. (A) UMAP of 22 identified clusters. (B) Comparison of 6 samples categorised into LP versus HP based on their parasitaemia quantified via microscopy of blood smears. (C) Relative abundance of cell types comparing samples ordered by parasitaemia as quantified via microscopy of blood smears. Abundance is colour-coded by a red colour scale (normalisation per row).

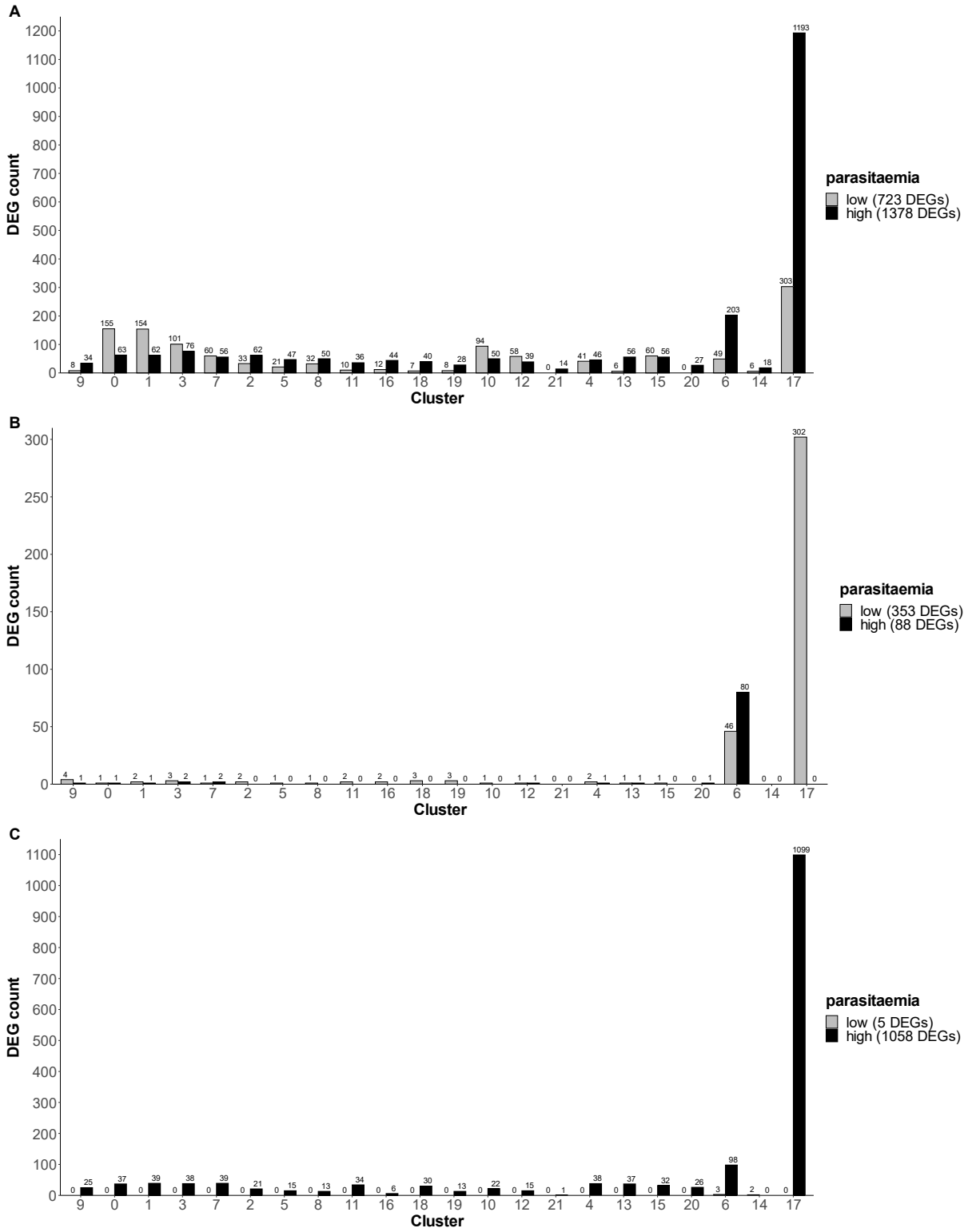

Figure 2: (A) Differentially expressed genes comparing LP versus HP per cluster (cut-off: p-value (adjusted) ≤ 0.05). (B) Strongly differentially expressed host genes (cut-off: p-value (adjusted) ≤ 0.05; log_2-FC (averaged) ≥ 1) comparing LP versus HP per cluster. Unannotated genes were omitted (C): Strongly differentially expressed parasite genes (cut-off: p-value (adjusted) ≤ 0.05; log_2-FC (averaged)

401 ≥ 1) comparing LP versus HP per cluster. Unannotated genes were omitted. Clusters are ordered by

402 cell type.

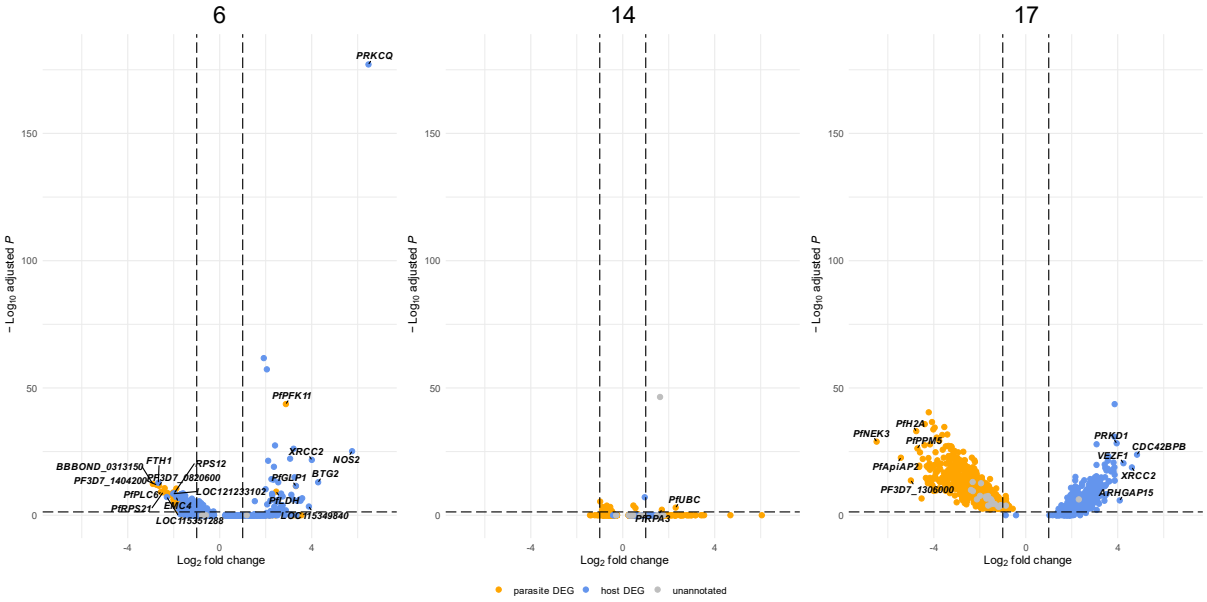

403

404 Figure 3: Differential gene expression across gametocyte clusters (top five host and parasite DEGs of

405 LP versus HP are labelled). Dotted lines delimit cut-off-values (p-value (adjusted) ≤ 0.05; log_2-FC

406 (averaged) ≥ 1). Negative and positive values for log_2-FC represent differential expression under HP

407 versus LP respectively.

408

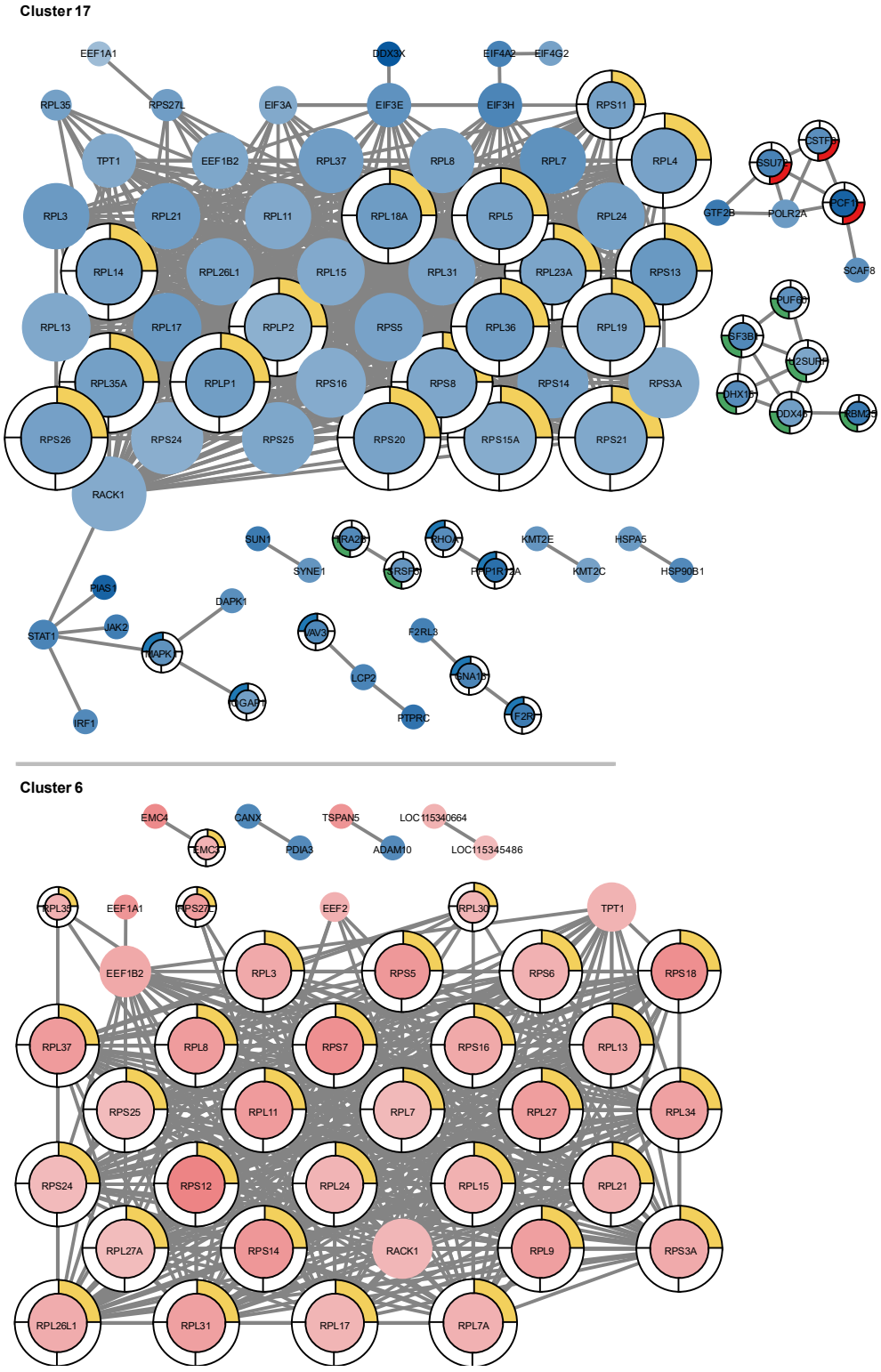

409

410 Figure 4: String PPI-networks of host genes (p-value (adjusted) ≤ 0.05; $\log_2$-FC (averaged) ≥ 1) of

411 developing gametocytes microgametocytes. Node colour intensity encodes differential expression

412 comparing LP (blue) versus HP (red). Colouring outside nodes refers to enriched KEGG pathways

413 (yellow: “ribosome” (False discovery rate (FDR) = 4.99E-36); red: “mRNA surveillance pathway” (FDR =

414 0.0451); green: “spliceosome” (FDR = 0.0047); blue: “regulation of actin cytoskeleton” (FDR = 0.0013)).

415 Node size corresponds to number of connections.

416 ## Extended Data Figures

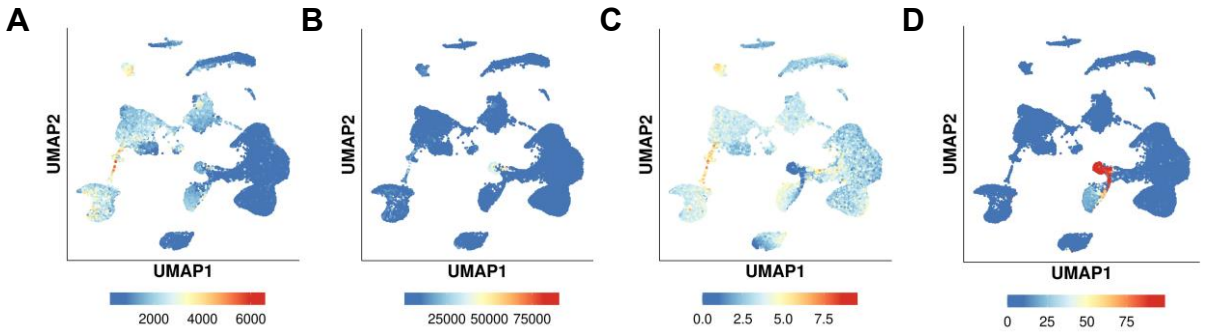

417

418 Figure S1: UMAPs displaying (A) number of genes expressed per cell, (B) number of UMIs detected per

419 cell, (C) proportion of mitochondrial genes per cell and (D) proportion of parasite genes per cell (genes

420 mapped to reference genomes of parasite species).

421

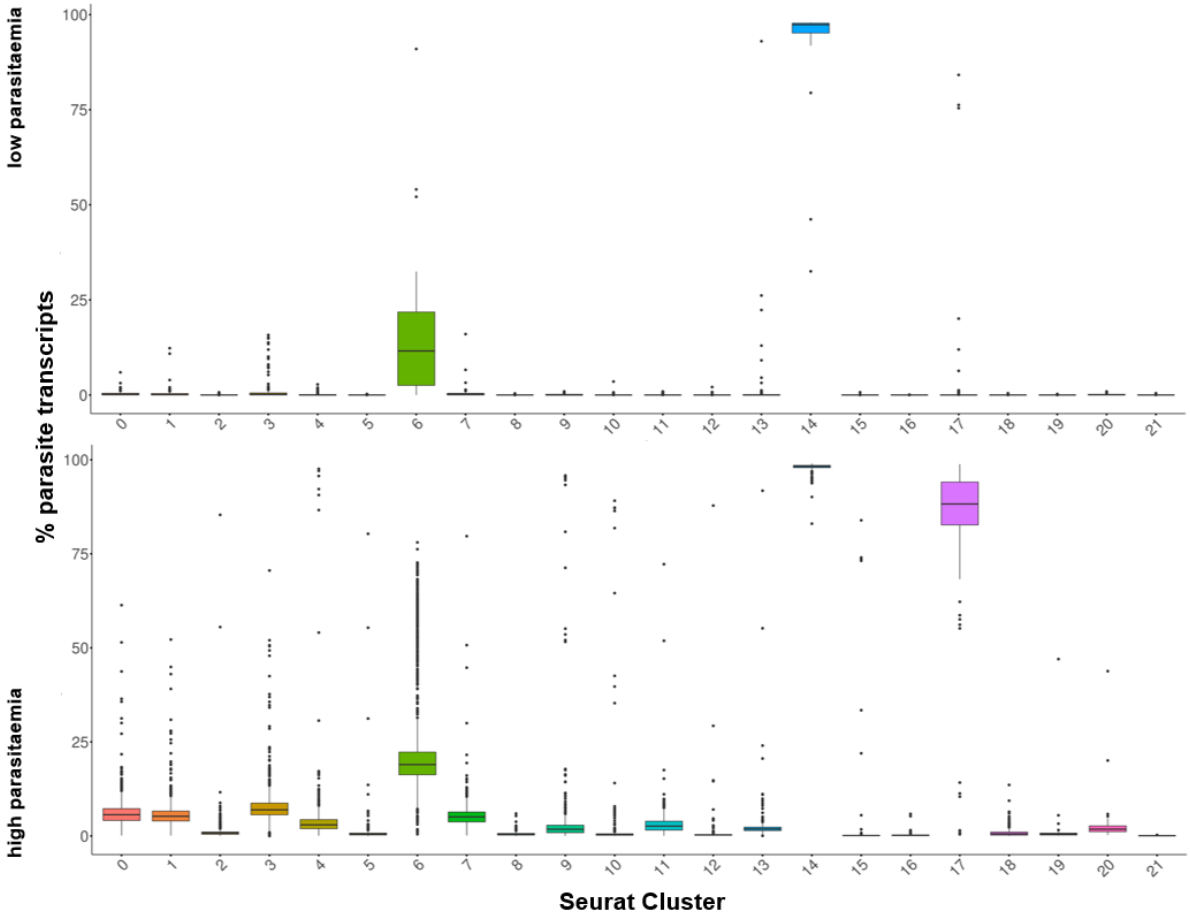

422

423 Figure S2: Proportion of parasite transcripts per cluster comparing low versus high parasitaemia.

424

red blood cells
thrombocytes
CD4+ T cell
CD8+ T cell
B cell
put. heterophil
put. eosinophil
put. monocyte
unannotated
put. microgametocyte
put. macrogametocyte
put. dev. gametocyte
Marker References
Cluster 9 0 1 3 7 2 5 8 11 16 18 19 10 12 21 4 13 15 20 6 14 17
[73]
Hemoglobin subunit α-A9
Hemoglobin subunit α-D9
Hemoglobin subunit β9
[74]
MPL (isoform X2)1, 3, 7
MPL (isoform X7)
GP9 7
ITGB30, 1, 3, 7
ITGB10, 1, 3, 7, 18
ITGA61, 3, 7
ITGA21, 3, 7
ITGAV4, 8, 11, 12, 13, 15, 16, 18, 20
F2R1, 3, 7
F2RL30, 1, 3, 7
P2RX1
P2RY1
HTR2A1, 6, 7
CD36
TBXAS11, 3, 4, 7, 13
GP1BA
[33]
CD3D2, 5, 8, 10, 11, 16, 18, 19
CD45, 8, 11, 16
IL7R2, 5, 8, 11, 19
CD285, 8, 16
CD8B18, 19
CD5
CD442, 4, 5, 8, 11, 13, 15, 16, 18, 19
BCL11A10, 12, 21
LOC115338201 10, 12, 15, 21
LOC115338202 10, 12, 15, 21
[76-77]
LOC115340258 (IL-8-like)
LOC115340259 (IL-8-like)1, 4, 7, 13, 15
IL18
GAL1
GAL313
GAL3
GAL7
LOC116441978 (GAL8-like)
GAL9
CTSB15
CTSD2, 4, 8, 12, 13, 15, 16, 18
CTSE
LOC115336252 (CTSEA-like)
CTSH12, 15
CTSK
CTSL
LOC115349310 (CTSL-like)4, 13, 18
CTSO
LOC115345557 (CTSS-like)15
CTSZ
LOC115334616 (LYZ-G-like)
LOC115334657 (LYZ-G-like, partial) 15
LOC115334707 (LYZ-G-like)
ACP2
ACP3
ACP5
ACP6
GUSB15
GAA
LOC115335647 (GAA-like)
LOC115335647 (GAA-like)
GANC
GANAB
Percent Expressed
0
25
50
75
Average Expression
6
4
2
0

426 Figure S3: Dotplot of host marker genes curated from literature[33,74–78]. Clusters were *o*rdered by
427 qualitative examination of marker gene expression under consideration of cluster distribution in Fig.
428 1A. Final annotations are indicated at the top of the plot. Annotations in superscript list clusters in
429 which a gene is differentially expressed in comparison to all clusters. Gene names in grey font
430 represent indirectly inferred markers (non-transcriptomic markers). Duplicates are based on two
431 transcript variants mapped to the same gene.

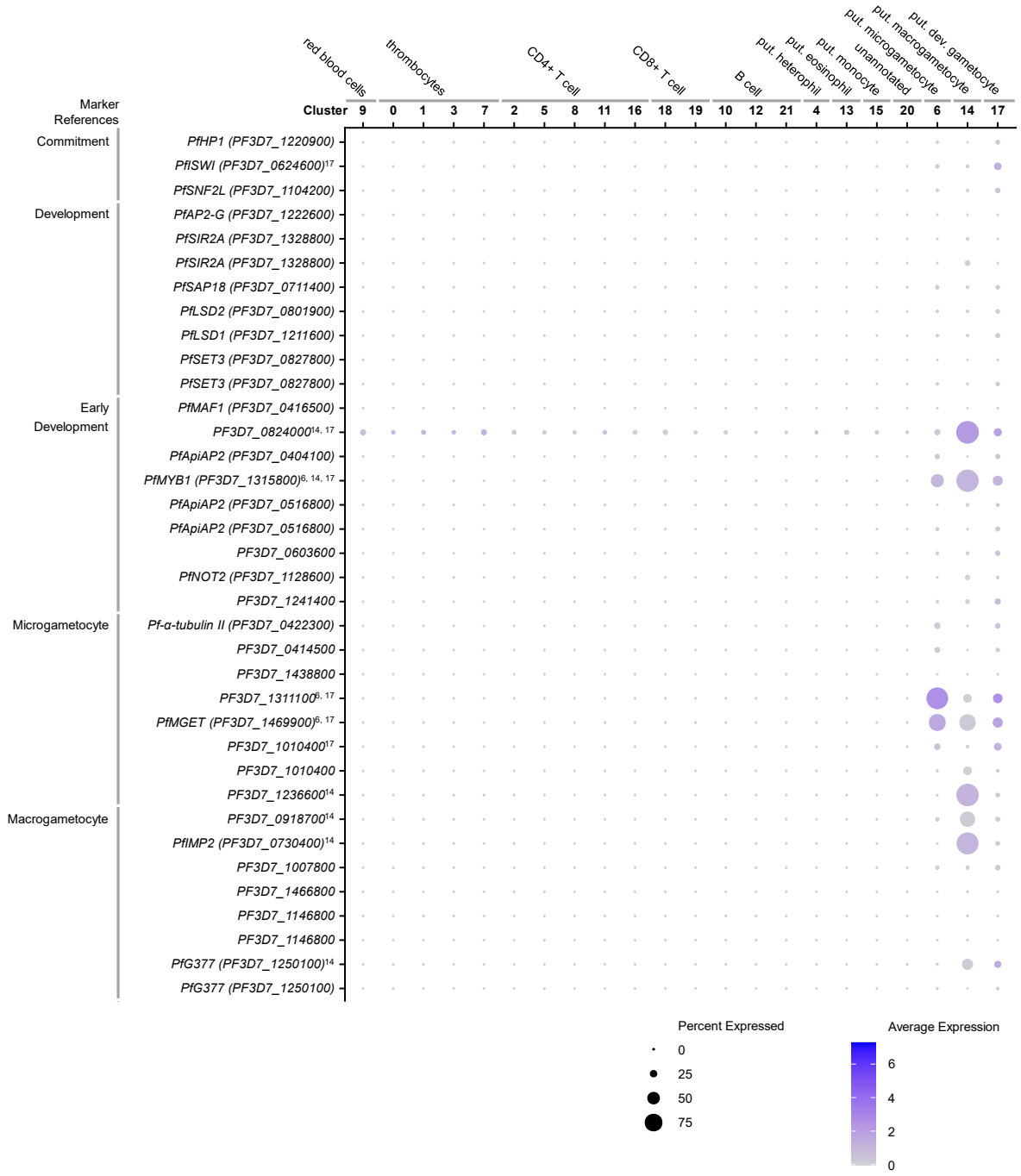

Figure S4: Dotplot of parasite marker genes from curated literature[79]. Clusters were ordered by qualitative examination of marker gene expression under consideration of cluster distribution in Fig. 1A. Final annotations are indicated at the top of the plot. Annotations in superscript list clusters in which a gene is differentially expressed in comparison to all clusters. Categories include commitment to gametocytogenesis (“commitment”) versus gametocytic development (“development”), early

gametocyte development and micro- and macrogametocyte specific markers. Duplicates are based on two transcript variants mapped to the same gene.

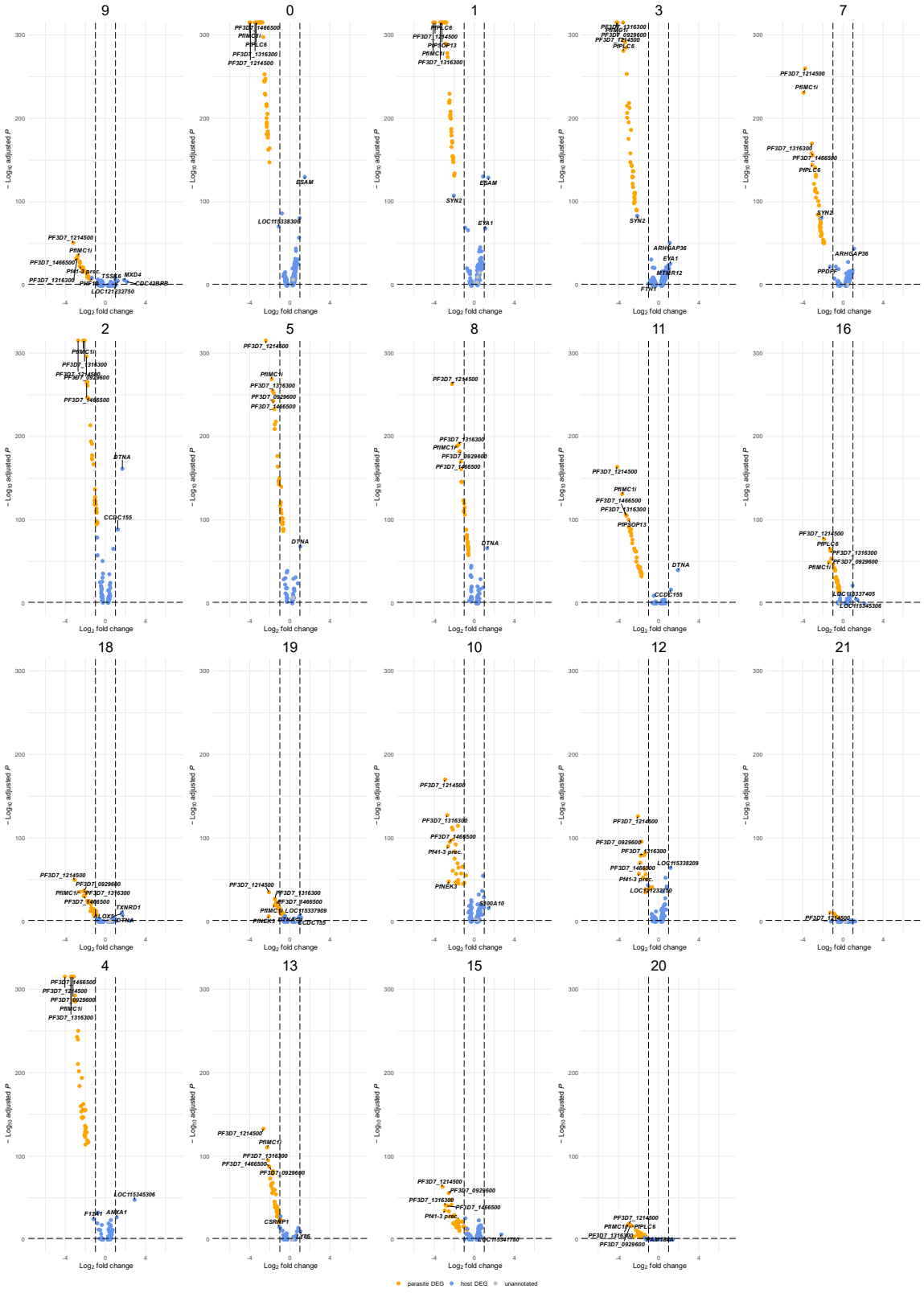

441 Figure S5: Differential gene expression across host clusters (top five host and parasite DEGs of LP versus
442 HP are labelled). Dotted lines delimit cut-off-values (p-value (adjusted) ≤ 0.05; log_2-FC (averaged) ≥ 1).
443 Negative and positive values for log_2-FC represent differential expression under HP versus LP
444 respectively. Clusters are ordered by cell type.

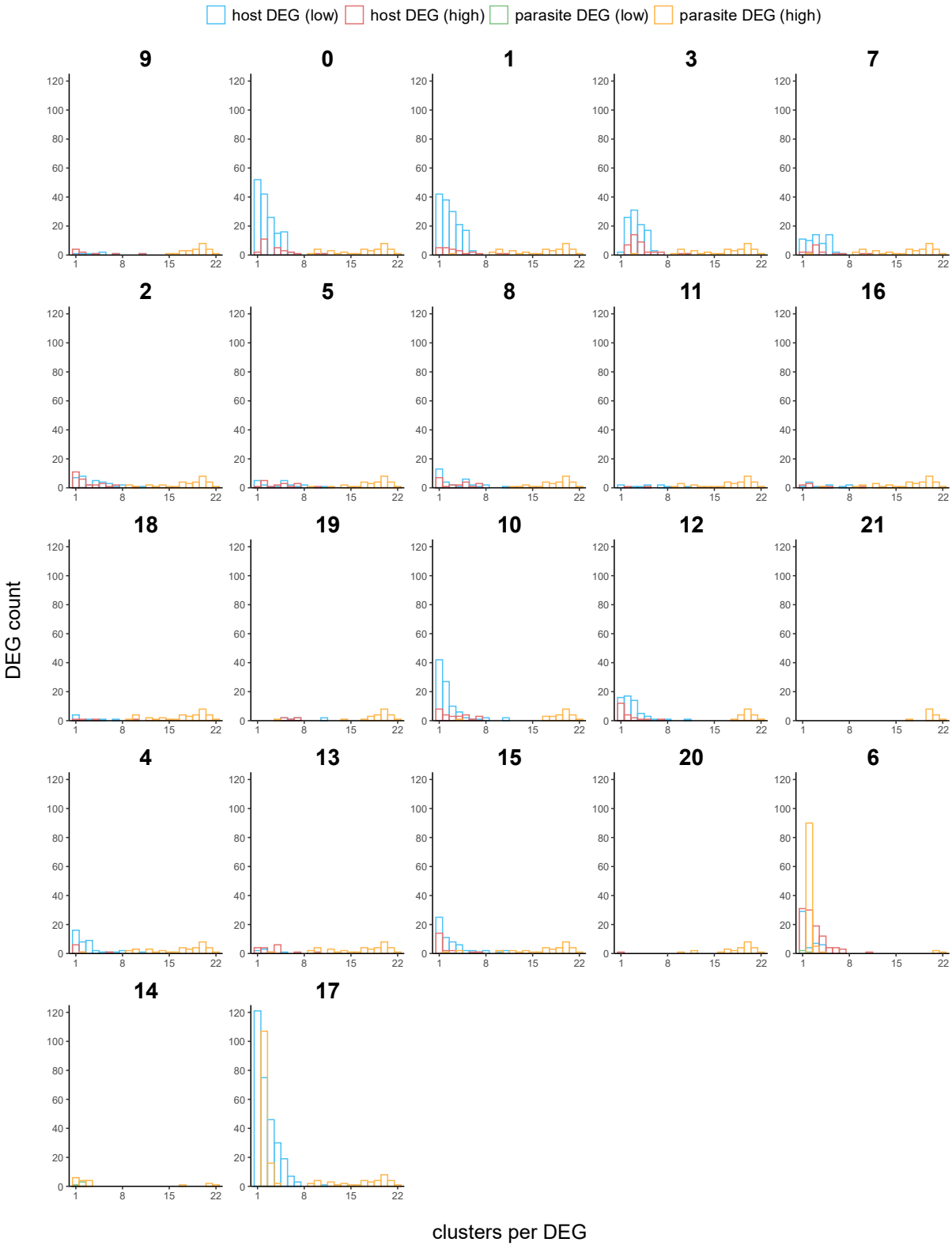

Figure S6: Redundancy of differentially expressed genes (cut-off: p-value (adjusted) ≤ 0.05). DEG counts are plotted against the number of clusters a gene is differentially expressed in. Unannotated genes were omitted.

449 ## References

450 1. Thompson JN. The coevolutionary process. Chicago: Univ. of Chicago Press 1994.

451 2. Windsor DA. Most of the species on Earth are parasites. Int J Parasitol 1998; 28: 1939–1941.

452 3. Schmid-Hempel P. Immune defence, parasite evasion strategies and their relevance for 'macroscopic
453 phenomena' such as virulence. Philos Trans R Soc Lond B Biol Sci 2009; 364: 85–98.

454 4. Ewald PW. Transmission modes and evolution of the parasitism-mutualism continuum. Ann N Y Acad
455 Sci 1987; 503: 295–306.

456 5. Anderson RM and May RM. Coevolution of hosts and parasites. Parasitology 1982; 85 (Pt 2): 411–
457 426.

458 6. Ewald PW. Host-Parasite Relations, Vectors, and the Evolution of Disease Severity. Annu. Rev. Ecol.
459 Syst. 1983; 14: 465–485.

460 7. Day T. Parasite transmission modes and the evolution of virulence. Evolution 2001; 55: 2389–2400.

461 8. Day T. The evolution of virulence in vector-borne and directly transmitted parasites. Theor Popul
462 Biol 2002; 62: 199–213.

463 9. Acevedo MA, Dillemuth FP, Flick AJ, et al. Virulence-driven trade-offs in disease transmission: A
464 meta-analysis. Evolution 2019; 73: 636–647.

465 10. Schmid-Hempel P. Variation in immune defence as a question of evolutionary ecology. Proc Biol Sci
466 2003; 270: 357–366.

467 11. Deroost K, Pham T-T, Opdenakker G, et al. The immunological balance between host and parasite
468 in malaria. FEMS Microbiol Rev 2016; 40: 208–257.

469 12. Zambrano-Villa S, Rosales-Borjas D, Carrero JC, et al. How protozoan parasites evade the immune
470 response. Trends Parasitol 2002; 18: 272–278.

471 13. Gomes PS, Bhardwaj J, Rivera-Correa J, et al. Immune Escape Strategies of Malaria Parasites. Front
472 Microbiol 2016; 7: 1617.

473 14. Rénia L and Goh YS. Malaria Parasites: The Great Escape. Front Immunol 2016; 7: 463.

474 15. Cowman AF, Tonkin CJ, Tham W-H, et al. The Molecular Basis of Erythrocyte Invasion by Malaria
475 Parasites. Cell Host Microbe 2017; 22: 232–245.

476 16. Rivero A and Gandon S. Evolutionary Ecology of Avian Malaria: Past to Present. Trends Parasitol
477 2018; 34: 712–726.

478 17. Pacheco MA, Matta NE, Valkiunas G, et al. Mode and Rate of Evolution of Haemosporidian
479 Mitochondrial Genomes: Timing the Radiation of Avian Parasites. Mol Biol Evol 2018; 35: 383–403.

480 18. Valkiūnas G. Avian malaria parasites and other haemosporidia. CRC Press 2005.

481 19. Harl J, Himmel T, Valkiūnas G, et al. Avian haemosporidian parasites of accipitriform raptors. Malar
482 J 2022; 21: 14.

483 20. Shutler D, Ankney CD and Mullie A. Effects of the blood parasite *Leucocytozoon simondi* on growth
484 rates of anatid ducklings. Can. J. Zool. 1999; 77: 1573–1578.

485 21. Wiegmann A, Springer A, Rinaud T, et al. The prevalence of *Leucocytozoon* spp. in nestlings of three
486 wild raptor species including implications on haematological and blood chemistry values. Int J Parasitol
487 Parasites Wildl 2021; 16: 236–243.

488 22. Rinaud T, Ottensmann M, Krüger O, et al. Acute blood parasite infections induce moderate
489 physiological costs in juvenile raptor hosts. EcoEvoRxiv 2022.

490 23. Ottensmann M, Wiegmann A, Krüger O, et al. Survival in a changing world: early life and weather
491 matter in a long-lived avian predator. in prep.

492 24. Ashford RW, Wyllie I and Newton I. *Leucocytozoon toddi* in British sparrowhawks *Accipiter nisus*
493 observations on the dynamics of infection. Journal of Natural History 1990; 24: 1101–1107.

494 25. Chakarov N, Linke B, Boerner M, et al. Apparent vector-mediated parent-to-offspring transmission
495 in an avian malaria-like parasite. Mol Ecol 2015; 24: 1355–1363.

496 26. Kaiser MI, Gadau J, Kaiser S, et al. Individualized social niches in animals: Theoretical clarifications
497 and processes of niche change. BioScience 2024.

498 27. Videvall E, Cornwallis CK, Palinauskas V, et al. The avian transcriptome response to malaria
499 infection. Mol Biol Evol 2015; 32: 1255–1267.

500 28. Outlaw DC, Walstrom VW, Bodden HN, et al. Molecular evolution in immune genes across the avian
501 tree of life. Parasitol Open 2019; 5.

502 29. Videvall E, Palinauskas V, Valkiūnas G, et al. Host Transcriptional Responses to High- and Low-
503 Virulent Avian Malaria Parasites. Am Nat 2020; 195: 1070–1084.

504 30. Kalbskopf V, Ahrén D, Valkiūnas G, et al. Shifts in gene expression variability in the blood-stage of
505 Plasmodium relictum. Gene 2021; 792: 145723.

506 31. Dai M, Zhao L, Li Z, et al. The Transcriptional Differences of Avian CD4(+)CD8(+) Double-Positive T
507 Cells and CD8(+) T Cells From Peripheral Blood of ALV-J Infected Chickens Revealed by Smart-Seq2.
508 Front Cell Infect Microbiol 2021; 11: 747094.

509 32. Liang Y, Ma Y, Zhang Y, et al. Single-Cell Analysis of the In Vivo Dynamics of Host Circulating Immune
510 Cells Highlights the Importance of Myeloid Cells in Avian Flaviviral Infection. J Immunol 2021; 207:
511 2878–2891.

512 33. Qu X, Li X, Li Z, et al. Chicken Peripheral Blood Mononuclear Cells Response to Avian Leukosis Virus
513 Subgroup J Infection Assessed by Single-Cell RNA Sequencing. Front Microbiol 2022; 13: 800618.

514 34. Bean AG and Lowenthal JW. Avian cytokines and their receptors. In: Avian Immunology (Third
515 Edition): Academic Press, 2022, pp. 249–276.

516 35. Popa GL and Popa MI. Recent Advances in Understanding the Inflammatory Response in Malaria:
517 A Review of the Dual Role of Cytokines. J Immunol Res 2021; 2021: 7785180.

518 36. Howick VM, Russell AJC, Andrews T, et al. The Malaria Cell Atlas: Single parasite transcriptomes
519 across the complete Plasmodium life cycle. Science 2019; 365.

520 37. Brandler T and Chakarov N. Mitochondrial and apicoplast genome copy abundances of
521 haemosporidian parasites are explained by host species and parasitic lineage. Front. Ecol. Evol. 2024;
522 12.

523 38. Mair GR, Braks JAM, Garver LS, et al. Regulation of sexual development of *Plasmodium* by
524 translational repression. Science 2006; 313: 667–669.

525 39. Groff TC, Lorenz TJ, Iezhova TA, et al. Description and molecular characterization of novel
526 *Leucocytozoon* parasite (Apicomplexa: Haemosporida: Leucocytozoidae), *Leucocytozoon polynuclearis*
527 n. sp. found in North American woodpeckers. Syst Parasitol 2022; 99: 103–114.

528 40. Chagas CRF, Duc M, Gutiérrez-Liberato GA, et al. Host Cells of *Leucocytozoon* (Haemosporida,
529 Leucocytozoidae) Gametocytes, with Remarks on the Phylogenetic Importance of This Character.
530 Pathogens 2023; 12.

531 41. Zhao W, Liu J, Xu R, et al. The Gametocytes of *Leucocytozoon sabrazesi* Infect Chicken
532 Thrombocytes, Not Other Blood Cells. PLoS One 2015; 10: e0133478.

533 42. Ferreira JL, Heincke D, Wichers JS, et al. The Dynamic Roles of the Inner Membrane Complex in the
534 Multiple Stages of the Malaria Parasite. Front Cell Infect Microbiol 2020; 10: 611801.

535 43. McGovern KE and Wilson EH. Role of Chemokines and Trafficking of Immune Cells in Parasitic
536 Infections. Curr Immunol Rev 2013; 9: 157–168.

537 44. Hakimi M-A and Bougdour A. *Toxoplasma*'s ways of manipulating the host transcriptome via
538 secreted effectors. Curr Opin Microbiol 2015; 26: 24–31.

539 45. Mahanta A, Ganguli P, Barah P, et al. Integrative Approaches to Understand the Mastery in
540 Manipulation of Host Cytokine Networks by Protozoan Parasites with Emphasis on *Plasmodium* and
541 *Leishmania* Species. Front Immunol 2018; 9: 296.

542 46. Takada H and Kurisaki A. Emerging roles of nucleolar and ribosomal proteins in cancer,
543 development, and aging. Cell Mol Life Sci 2015; 72: 4015–4025.

544 47. Warncke JD and Beck H-P. Host Cytoskeleton Remodeling throughout the Blood Stages of
545 *Plasmodium falciparum*. Microbiol Mol Biol Rev 2019; 83.

546 48. Villares M, Berthelet J and Weitzman JB. The clever strategies used by intracellular parasites to
547 hijack host gene expression. Semin Immunopathol 2020; 42: 215–226.

548 49. Nájera CA, Batista MF, Meneghelli I, et al. Mixed signals - how *Trypanosoma cruzi* exploits host-cell
549 communication and signaling to establish infection. J Cell Sci 2021; 134.

550 50. Matulova M, Rajova J, Vlasatikova L, et al. Characterization of chicken spleen transcriptome after
551 infection with *Salmonella enterica* serovar Enteritidis. PLoS One 2012; 7: e48101.

552 51. Matulova M, Varmuzova K, Sisak F, et al. Chicken innate immune response to oral infection with
553 *Salmonella enterica* serovar Enteritidis. Vet Res 2013; 44: 37.

554 52. Meitern R, Andreson R and Hõrak P. Profile of whole blood gene expression following immune
555 stimulation in a wild passerine. BMC Genomics 2014; 15: 533.

556 53. Lüder CG, Lang T, Beuerle B, et al. Down-regulation of MHC class II molecules and inability to up-
557 regulate class I molecules in murine macrophages after infection with *Toxoplasma gondii*. Clin Exp
558 Immunol 1998; 112: 308–316.

559 54. Reiner NE, Ng W and McMaster WR. Parasite-accessory cell interactions in murine leishmaniasis.
560 II. *Leishmania donovani* suppresses macrophage expression of class I and class II major
561 histocompatibility complex gene products. J Immunol 1987; 138: 1926–1932.

562 55. Reiner NE, Ng W, Ma T, et al. Kinetics of gamma interferon binding and induction of major
563 histocompatibility complex class II mRNA in *Leishmania*-infected macrophages. Proc Natl Acad Sci U S
564 A 1988; 85: 4330–4334.

565 56. Lüder CGK, Walter W, Beuerle B, et al. *Toxoplasma gondii* down-regulates MHC class II gene
566 expression and antigen presentation by murine macrophages via interference with nuclear
567 translocation of STAT1α. Eur. J. Immunol. 2001; 31: 1475–1484.

568 57. Chakarov N, Pauli M and Krüger O. Immune responses link parasite genetic diversity, prevalence
569 and plumage morphs in common buzzards. Evol Ecol 2017; 31: 51–62.

570 58. Nakamori M and Takahashi MP. The role of α-dystrobrevin in striated muscle. Int J Mol Sci 2011;
571 12: 1660–1671.

572 59. Morimoto A, Shibuya H, Zhu X, et al. A conserved KASH domain protein associates with telomeres,
573 SUN1, and dynactin during mammalian meiosis. J Cell Biol 2012; 198: 165–172.

574 60. González-Granado JM, Silvestre-Roig C, Rocha-Perugini V, et al. Nuclear envelope lamin-A couples
575 actin dynamics with immunological synapse architecture and T cell activation. Sci Signal 2014; 7: ra37.

576 61. Zhang J, Wang Y, Chu Y, et al. Agrin is involved in lymphocytes activation that is mediated by alpha-
577 dystroglycan. FASEB J 2006; 20: 50–58.

578 62. Muri J, Heer S, Matsushita M, et al. The thioredoxin-1 system is essential for fueling DNA synthesis
579 during T-cell metabolic reprogramming and proliferation. Nat Commun 2018; 9: 1851.

580 63. Lüder CGK, Algner M, Lang C, et al. Reduced expression of the inducible nitric oxide synthase after
581 infection with *Toxoplasma gondii* facilitates parasite replication in activated murine macrophages. Int
582 J Parasitol 2003; 33: 833–844.

583 64. Calegari-Silva TC, Vivarini ÁC, Pereira RdMS, et al. *Leishmania amazonensis* downregulates
584 macrophage iNOS expression via Histone Deacetylase 1 (HDAC1): a novel parasite evasion mechanism.
585 Eur. J. Immunol. 2018; 48: 1188–1198.

586 65. Brunet LR. Nitric oxide in parasitic infections. Int Immunopharmacol 2001; 1: 1457–1467.

587 66. Ascenzi P, Bocedi A and Gradoni L. The anti-parasitic effects of nitric oxide. IUBMB Life 2003; 55:
588 573–578.

589 67. Sobolewski P, Gramaglia I, Frangos J, et al. Nitric oxide bioavailability in malaria. Trends Parasitol
590 2005; 21: 415–422.

591 68. Gozzelino R, Andrade BB, Larsen R, et al. Metabolic adaptation to tissue iron overload confers
592 tolerance to malaria. Cell Host Microbe 2012; 12: 693–704.

593 69. Ben-Othman R, Flannery AR, Miguel DC, et al. *Leishmania*-mediated inhibition of iron export
594 promotes parasite replication in macrophages. PLoS Pathog 2014; 10: e1003901.

595 70. Butler A, Hoffman P, Smibert P, et al. Integrating single-cell transcriptomic data across different
596 conditions, technologies, and species. Nat Biotechnol 2018; 36: 411–420.

597 71. Stuart T, Butler A, Hoffman P, et al. Comprehensive Integration of Single-Cell Data. Cell 2019; 177:
598 1888-1902.e21.

599 72. Hao Y, Hao S, Andersen-Nissen E, et al. Integrated analysis of multimodal single-cell data. Cell 2021;
600 184: 3573-3587.e29.

601 73. McGinnis CS, Murrow LM and Gartner ZJ. DoubletFinder: Doublet Detection in Single-Cell RNA
602 Sequencing Data Using Artificial Nearest Neighbors. Cell Syst 2019; 8: 329-337.e4.

603 74. Scanes CG. Sturkie's Avian Physiology - Sixth Edition - Chapter 10 - Blood 2015: 167–191.

604 75. Schmaier AA, Stalker TJ, Runge JJ, et al. Occlusive thrombi arise in mammals but not birds in
605 response to arterial injury: evolutionary insight into human cardiovascular disease. Blood 2011; 118:
606 3661–3669.

607 76. van Dijk A, Veldhuizen EJA and Haagsman HP. Avian defensins. Vet Immunol Immunopathol 2008;
608 124: 1–18.

609 77. Swaggerty CL, Kogut MH, Ferro PJ, et al. Differential cytokine mRNA expression in heterophils
610 isolated from *Salmonella*-resistant and -susceptible chickens. Immunology 2004; 113: 139–148.

611 78. Harmon BG. Avian heterophils in inflammation and disease resistance. Poult Sci 1998; 77: 972–977.

612 79. van Biljon R, van Wyk R, Painter HJ, et al. Hierarchical transcriptional control regulates *Plasmodium*
613 *falciparum* sexual differentiation. BMC Genomics 2019; 20: 920.

614 80. R Core Team. A language and environment for statistical computing 2021, https://www.R-
615 project.org/ (2021).

616 81. Shannon P, Markiel A, Ozier O, et al. Cytoscape: a software environment for integrated models of
617 biomolecular interaction networks. Genome Research 2003; 2498–2504.

618 82. Szklarczyk D, Gable AL, Lyon D, et al. STRING v11: protein-protein association networks with
619 increased coverage, supporting functional discovery in genome-wide experimental datasets. Nucleic
620 Acids Res 2019; 47: D607-D613.

621 83. Doncheva NT, Morris JH, Holze H, et al. Cytoscape stringApp 2.0: Analysis and Visualization of
622 Heterogeneous Biological Networks. J Proteome Res 2022.

623 84. Lessard J, Wu JI, Ranish JA, et al. An essential switch in subunit composition of a chromatin
624 remodeling complex during neural development. Neuron 2007; 55: 201–215.

625 85. Spiridonov NA, Wong L, Zerfas PM, et al. Identification and characterization of SSTK, a
626 serine/threonine protein kinase essential for male fertility. Mol Cell Biol 2005; 25: 4250–4261.

627 86. Boros K, Lacaud G and Kouskoff V. The transcription factor Mxd4 controls the proliferation of the
628 first blood precursors at the onset of hematopoietic development in vitro. Exp Hematol 2011; 39:
629 1090–1100.

630 87. Vasilevsky NA, Ruby CE, Hurlin PJ, et al. OX40 engagement stabilizes Mxd4 and Mnt protein levels
631 in antigen-stimulated T cells leading to an increase in cell survival. Eur J Immunol 2011; 41: 1024–1034.

632 88. Leung T, Chen XQ, Tan I, et al. Myotonic dystrophy kinase-related Cdc42-binding kinase acts as a
633 Cdc42 effector in promoting cytoskeletal reorganization. Mol Cell Biol 1998; 18: 130–140.

634 89. Neefjes J, Jongsma MLM, Paul P, et al. Towards a systems understanding of MHC class I and MHC
635 class II antigen presentation. Nat Rev Immunol 2011; 11: 823–836.

636 90. Nasdala I, Wolburg-Buchholz K, Wolburg H, et al. A transmembrane tight junction protein
637 selectively expressed on endothelial cells and platelets. J Biol Chem 2002; 277: 16294–16303.

638 91. Wegmann F, Petri B, Khandoga AG, et al. ESAM supports neutrophil extravasation, activation of
639 Rho, and VEGF-induced vascular permeability. J Exp Med 2006; 203: 1671–1677.

640 92. Greengard P, Valtorta F, Czernik AJ, et al. Synaptic vesicle phosphoproteins and regulation of
641 synaptic function. Science 1993; 259: 780–785.

642 93. Bhangu PS, Genever PG, Spencer GJ, et al. Evidence for targeted vesicular glutamate exocytosis in
643 osteoblasts. Bone 2001; 29: 16–23.

644 94. Maiole F, Tedeschi G, Candiani S, et al. Synapsins are expressed at neuronal and non-neuronal
645 locations in Octopus vulgaris. Sci Rep 2019; 9: 15430.

646 95. Cook PJ, Ju BG, Telese F, et al. Tyrosine dephosphorylation of H2AX modulates apoptosis and
647 survival decisions. Nature 2009; 458: 591–596.

648 96. Krishnan N, Jeong DG, Jung S-K, et al. Dephosphorylation of the C-terminal tyrosyl residue of the
649 DNA damage-related histone H2A.X is mediated by the protein phosphatase eyes absent. J Biol Chem
650 2009; 284: 16066–16070.

651 97. Hegde RS, Roychoudhury K and Pandey RN. The multi-functional eyes absent proteins. Crit Rev
652 Biochem Mol Biol 2020; 55: 372–385.

653 98. Nandurkar HH, Caldwell KK, Whisstock JC, et al. Characterization of an adapter subunit to a
654 phosphatidylinositol (3)P 3-phosphatase: identification of a myotubularin-related protein lacking
655 catalytic activity. Proc Natl Acad Sci U S A 2001; 98: 9499–9504.

656 99. Nandurkar HH, Layton M, Laporte J, et al. Identification of myotubularin as the lipid phosphatase
657 catalytic subunit associated with the 3-phosphatase adapter protein, 3-PAP. Proc Natl Acad Sci U S A
658 2003; 100: 8660–8665.

659 100. Hnia K, Vaccari I, Bolino A, et al. Myotubularin phosphoinositide phosphatases: cellular functions
660 and disease pathophysiology. Trends Mol Med 2012; 18: 317–327.

661 101. Fagerberg L, Hallström BM, Oksvold P, et al. Analysis of the human tissue-specific expression by
662 genome-wide integration of transcriptomics and antibody-based proteomics. Mol Cell Proteomics
663 2014; 13: 397–406.

664 102. Nam H, Jeon S, An H, et al. Critical roles of ARHGAP36 as a signal transduction mediator of Shh
665 pathway in lateral motor columnar specification. eLife 2019; 8.

666 103. Comer SP. Turning Platelets Off and On: Role of RhoGAPs and RhoGEFs in Platelet Activity. Front
667 Cardiovasc Med 2021; 8: 820945.

668 104. Jiang Z, Song J, Qi F, et al. Exdpf is a key regulator of exocrine pancreas development controlled
669 by retinoic acid and ptf1a in zebrafish. PLoS Biol 2008; 6: e293.

670 105. Yun M, Yingzi L, Jie G, et al. PPDPF Promotes the Progression and acts as an Antiapoptotic Protein
671 in Non-Small Cell Lung Cancer. Int J Biol Sci 2022; 18: 214–228.

672 106. Tuohimaa P, Joensuu T, Isola J, et al. Development of progestin-specific response in the chicken
673 oviduct. Int J Dev Biol 1989; 33: 125–134.

674 107. Loes AN, Bridgham JT and Harms MJ. Coevolution of the Toll-Like Receptor 4 Complex with
675 Calgranulins and Lipopolysaccharide. Front Immunol 2018; 9: 304.

676 108. Cook-Moreau JM, El-Makhour Hojeij Y, Barrière G, et al. Expression of 5-lipoxygenase (5-LOX) in
677 T lymphocytes. Immunology 2007; 122: 157–166.

678 109. Lone AM and Taskén K. Proinflammatory and immunoregulatory roles of eicosanoids in T cells.
679 Front Immunol 2013; 4: 130.

680 110. Sun Q-Y, Zhou H-H and Mao X-Y. Emerging Roles of 5-Lipoxygenase Phosphorylation in
681 Inflammation and Cell Death. Oxidative Medicine and Cellular Longevity 2019; 2019: 2749173.

682 111. Lanier LL. NKG2D Receptor and Its Ligands in Host Defense. Cancer Immunol Res 2015; 3: 575–
683 582.

684 112. Lou Y, Han M, Liu H, et al. Essential roles of S100A10 in Toll-like receptor signaling and immunity
685 to infection. Cell Mol Immunol 2020; 17: 1053–1062.

686 113. Francischetti IMB, Seydel KB and Monteiro RQ. Blood coagulation, inflammation, and malaria.
687 Microcirculation 2008; 15: 81–107.

688 114. Sheikh MH and Solito E. Annexin A1: Uncovering the Many Talents of an Old Protein. Int J Mol Sci
689 2018; 19.

690 115. Pang J, Yu Q, Chen Y, et al. Integrating Single-cell RNA-seq to construct a Neutrophil prognostic
691 model for predicting immune responses in non-small cell lung cancer. J Transl Med 2022; 20: 531.

692 116. Schultz TE and Blumenthal A. The RP105/MD-1 complex: molecular signaling mechanisms and
693 pathophysiological implications. J Leukoc Biol 2017; 101: 183–192.

694 117. Sancho D and Reis e Sousa C. Signaling by myeloid C-type lectin receptors in immunity and
695 homeostasis. Annu Rev Immunol 2012; 30: 491–529.

696 118. Liu L, Lin J and He H. Identification of Potential Crucial Genes Associated With the Pathogenesis
697 and Prognosis of Endometrial Cancer. Front Genet 2019; 10: 373.

698 119. Huang W, Li G, Wang Z, et al. A Ten-N6-Methyladenosine (m6A)-Modified Gene Signature Based
699 on a Risk Score System Predicts Patient Prognosis in Rectum Adenocarcinoma. Front Oncol 2020; 10:
700 567931.

701 120. Xing J, Shen S, Liu X, et al. A hypoxia-related prognostic model predicts overall survival and
702 treatment response in hepatocellular carcinoma. Biosci Rep 2022; 42.

703 121. Meister A and Anderson ME. Glutathione. Annu Rev Biochem 1983; 52: 711–760.

704 122. Brown GD, Willment JA and Whitehead L. C-type lectins in immunity and homeostasis. Nat Rev
705 Immunol 2018; 18: 374–389.

706 123. Jonikas MC, Collins SR, Denic V, et al. Comprehensive characterization of genes required for
707 protein folding in the endoplasmic reticulum. Science 2009; 323: 1693–1697.

708 124. Shurtleff MJ, Itzhak DN, Hussmann JA, et al. The ER membrane protein complex interacts
709 cotranslationally to enable biogenesis of multipass membrane proteins. eLife 2018; 7.

710 125. Verdot L, Lalmanach G, Vercruysse V, et al. Cystatins up-regulate nitric oxide release from
711 interferon-gamma-activated mouse peritoneal macrophages. J Biol Chem 1996; 271: 28077–28081.

712 126. Das L, Datta N, Bandyopadhyay S, et al. Successful therapy of lethal murine visceral leishmaniasis
713 with cystatin involves up-regulation of nitric oxide and a favorable T cell response. J Immunol 2001;
714 166: 4020–4028.

715 127. Hartmann S, Schönemeyer A, Sonnenburg B, et al. Cystatins of filarial nematodes up-regulate the
716 nitric oxide production of interferon-gamma-activated murine macrophages. Parasite immunology
717 2002; 24: 253–262.

718 128. Johnson RD, Liu N and Jasin M. Mammalian XRCC2 promotes the repair of DNA double-strand
719 breaks by homologous recombination. Nature 1999; 401: 397–399.

720 129. Deans B, Griffin CS, Maconochie M, et al. Xrcc2 is required for genetic stability, embryonic
721 neurogenesis and viability in mice. EMBO J 2000; 19: 6675–6685.

722 130. Yuniati L, Scheijen B, van der Meer LT, et al. Tumor suppressors BTG1 and BTG2: Beyond growth
723 control. J Cell Physiol 2019; 234: 5379–5389.

724 131. Damena D, Agamah FE, Kimathi PO, et al. Insilico Functional Analysis of Genome-Wide Dataset
725 From 17,000 Individuals Identifies Candidate Malaria Resistance Genes Enriched in Malaria Pathogenic
726 Pathways. Front Genet 2021; 12: 676960.

727 132. Cohen S, Braiman A, Shubinsky G, et al. Protein kinase C-theta in platelet activation. FEBS Lett
728 2011; 585: 3208–3215.

729 133. Ivison SM, Graham NR, Bernales CQ, et al. Protein kinase D interaction with TLR5 is required for
730 inflammatory signaling in response to bacterial flagellin. J Immunol 2007; 178: 5735–5743.

731 134. Zhang X, Connelly J, Chao Y, et al. Multifaceted Functions of Protein Kinase D in Pathological
732 Processes and Human Diseases. Biomolecules 2021; 11.

733 135. Bosco EE, Mulloy JC and Zheng Y. Rac1 GTPase: a "Rac" of all trades. Cell Mol Life Sci 2009; 66:
734 370–374.

735 136. Xiong JW, Leahy A, Lee HH, et al. Vezf1: A Zn finger transcription factor restricted to endothelial
736 cells and their precursors. Dev Biol 1999; 206: 123–141.

737 137. Niu J, Qin B, Wang C, et al. Identification of Key Immune-Related Genes in the Progression of
738 Septic Shock. Front Genet 2021; 12: 668527.

739 138. Ravel DB. Mechanisms of Cellular Remodeling during *Plasmodium falciparum* Sequestration and
740 Transmission 2017; Doctoral dissertation, Harvard University, Graduate School of.

741 139. Vaid A and Sharma P. PfPKB, a protein kinase B-like enzyme from *Plasmodium falciparum*: II.
742 Identification of calcium/calmodulin as its upstream activator and dissection of a novel signaling
743 pathway. J Biol Chem 2006; 281: 27126–27133.

744 140. Vaid A, Thomas DC and Sharma P. Role of Ca2+/calmodulin-PfPKB signaling pathway in
745 erythrocyte invasion by *Plasmodium falciparum*. J Biol Chem 2008; 283: 5589–5597.

746 141. Ecker A, Bushell ESC, Tewari R, et al. Reverse genetics screen identifies six proteins important for
747 malaria development in the mosquito. Mol Microbiol 2008; 70: 209–220.

748 142. Lye YM, Chan M and Sim T-S. Pfnek3: an atypical activator of a MAP kinase in *Plasmodium*
749 *falciparum*. FEBS Lett 2006; 580: 6083–6092.

750 143. Capelli-Peixoto J, Saelao P, Johnson WC, et al. Comparison of high throughput RNA sequences
751 between *Babesia bigemina* and *Babesia bovis* revealed consistent differential gene expression that is
752 required for the *Babesia* life cycle in the vertebrate and invertebrate hosts. Front Cell Infect Microbiol
753 2022; 12: 1093338.

754 144. Boucher MJ, Ghosh S, Zhang L, et al. Integrative proteomics and bioinformatic prediction enable
755 a high-confidence apicoplast proteome in malaria parasites. PLoS Biol 2018; 16: e2005895.

756 145. Wong W, Bai X, Brown A, et al. Cryo-EM structure of the *Plasmodium falciparum* 80S ribosome
757 bound to the anti-protozoan drug emetine. eLife 2014; 3.

758 146. Bzik DJ, Fox BA and Gonyer K. Expression of *Plasmodium falciparum* lactate dehydrogenase in
759 Escherichia coli. Mol Biochem Parasitol 1993; 59: 155–166.

760 147. Makler MT and Hinrichs DJ. Measurement of the lactate dehydrogenase activity of *Plasmodium*
761 *falciparum* as an assessment of parasitemia. Am J Trop Med Hyg 1993; 48: 205–210.

762 148. Mony BM, Mehta M, Jarori GK, et al. Plant-like phosphofructokinase from *Plasmodium falciparum*
763 belongs to a novel class of ATP-dependent enzymes. Int J Parasitol 2009; 39: 1441–1453.

764 149. Rahlfs S, Fischer M and Becker K. *Plasmodium falciparum* possesses a classical glutaredoxin and a
765 second, glutaredoxin-like protein with a PICOT homology domain. J Biol Chem 2001; 276: 37133–
766 37140.

767 150. Tajedin L, Anwar M, Gupta D, et al. Comparative insight into nucleotide excision repair
768 components of *Plasmodium falciparum*. DNA Repair (Amst) 2015; 28: 60–72.

769 151. Chung D-WD, Ponts N, Prudhomme J, et al. Characterization of the ubiquitylating components of
770 the human malaria parasite's protein degradation pathway. PLoS One 2012; 7: e43477.

771 152. Goyal M, Heinberg A, Mitesser V, et al. Phosphorylation of the Canonical Histone H2A Marks Foci
772 of Damaged DNA in Malaria Parasites. mSphere 2021; 6.

773 153. Guttery DS, Poulin B, Ramaprasad A, et al. Genome-wide functional analysis of *Plasmodium*
774 protein phosphatases reveals key regulators of parasite development and differentiation. Cell Host
775 Microbe 2014; 16: 128–140.